

## Recent advances of conjugated microporous polymers for photocatalysis: designs, applications, and perspectives

Songhao Luo, <sup>†a</sup> Zhuotong Zeng, <sup>†b</sup> Guangming Zeng, <sup>\*</sup> Zhifeng Liu, <sup>\*</sup> Rong Xiao, <sup>\*</sup> Piao Xu, <sup>a</sup> Han Wang, <sup>a</sup> Danlian Huang, <sup>a</sup> Yang Liu, <sup>a</sup> Binbin Shao, <sup>a</sup> Qinghua Liang, <sup>a</sup> Dongbo Wang, <sup>a</sup> Qingyun He, <sup>a</sup> Lei Qin <sup>a</sup> and Yukui Fu <sup>a</sup>

Received 00th January 20xx,  
Accepted 00th January 20xx

DOI: 10.1039/x0xx00000x

Solar energy is a clean and sustainable energy source. Nature photosynthesis has existed for millions of years, which can convert solar energy into the chemical energy needed by living things. Inspired by natural photosynthesis, scientists have developed a series of artificial photosynthetic systems that are eager to use solar energy efficiently for humans. Conjugated microporous polymers (CMPs) are a new class of materials that can be used in artificial photosynthetic systems. This review illustrates the light-harvesting capability and the energy transfer phenomena within the supramolecular structure of CMPs to provide guidelines for the rational design of these polymers with excellent photocatalytic properties, as well as systematically discusses the applications of these materials in the field of photocatalysis including photocatalytic water splitting, CO<sub>2</sub> reduction, organic conversion, environmental remediation, and medical health. Finally, this review points out the major challenges in this topic and suggests the next feasible development direction.

### 1. Introduction

Since the industrial revolution, the average living standard of human beings has increased, and the demand for energy has also grown rapidly. Energy is one of the key factors determining social and economic development, especially in developing countries. At present, the main energy used in the world is fossil energy.<sup>1-3</sup> They have two main shortcomings: (i) their limited earth storage cannot support the long-term high-speed development of human beings; (ii) the massive use of fossil energy has a negative impact on the environment. Therefore, it is necessary to explore new energy sources to provide new solutions for global development. Solar energy is widely considered to be a low-cost, clean and abundant source of energy.<sup>4-6</sup> The solar energy received on Earth is much higher than the human demand for energy. The use of solar energy is undoubtedly an effective strategy to improve the energy structure and improve the global ecological environment. The question now is how to efficiently convert solar energy into a chemical energy source for human use.

Photosynthesis, also known as photo energy synthesis, refers to convert solar energy into chemical energy by photosynthetic pigments or some natural photocatalysts in photosynthetic organisms under visible light irradiation. This unique biochemical process has existed in nature for millions of years. Inspired by natural photosynthesis, researchers have innovatively developed a range of artificial systems and devices that use organic and inorganic materials

to simulate natural photosynthesis.<sup>7-13</sup> They provide an effective way to convert solar energy into chemical energy.

The first successful attempt to convert solar energy into chemical energy occurred in 1972 when Fujishima and Honda found that TiO<sub>2</sub> electrodes could promote photocatalytic water decomposition.<sup>14</sup> As early as 2008, Fujishima reviewed the origin of TiO<sub>2</sub> photocatalyst based on the information available at the time and pointed out the potential development direction.<sup>15</sup> With the development of photocatalysis technologies, other materials have also attracted the attention of scientists. For example, mature transition metal complexes have been developed in recent years.<sup>16-22</sup> In addition, there are other hot metal-free and semiconductor materials,<sup>23, 24</sup> such as graphene,<sup>25</sup> reduced graphene oxides,<sup>26-28</sup> g-C<sub>3</sub>N<sub>4</sub>,<sup>29-33</sup> and polyoxometalates (POMs).<sup>34-36</sup> However, these materials have some disadvantages which are difficult to solve: (i) they are unstable, and short in-service life; (ii) most noble metal materials are expensive and have low reserves in nature; (iii) these catalysts are extremely toxic to the ecological environment; (iv) they will be corroded by the reaction solvent in the reaction medium, thereby affecting the performance of the catalyst after recovery. Therefore, it is necessary to develop more types of heterogeneous photocatalysts with high stability and reusability.<sup>37-40</sup>

Recently, scientists have extensively studied the existing nanoporous heterogeneous catalytic materials.<sup>41, 42</sup> The nanometer properties help to achieve higher specific surface area,<sup>43, 44</sup> and the porous properties help to provide additional catalytic active sites.<sup>45-47</sup> Plasmon metal nanomaterials have surface plasmon resonance (SPR) properties, which give them the unique ability to collect electromagnetic fields and convert photon energy into heat energy, showing great application potential in the field of photocatalysis.<sup>48</sup> Owing to their regularity and synthesis of adjustable structure, metal organic framework (MOFs) can contain photosensitizer and catalytic center in single structure, and provide the channel structure to promote the spread of the substrate and product. As a light-

<sup>a</sup> College of Environmental Science and Engineering, Hunan University and Key Laboratory of Environmental Biology and Pollution Control (Hunan University), Ministry of Education, Changsha 410082, P.R. China. E-mail: [zgming@hnu.edu.cn](mailto:zgming@hnu.edu.cn) (G. Zeng) and [zhifengliu@hnu.edu.cn](mailto:zhifengliu@hnu.edu.cn) (Z. Liu)

<sup>b</sup> Department of Dermatology, Second Xiangya Hospital, Central South University, Changsha 410011, P. R. China. E-mail: [xiaorong65@csu.edu.cn](mailto:xiaorong65@csu.edu.cn) (R. Xiao)

<sup>†</sup> These authors contributed equally to this work.

Electronic Supplementary Information (ESI) available: [details of any supplementary information available should be included here]. See DOI: 10.1039/x0xx00000x

harvesting antenna and catalytic center, they have been proved to be quite effective in light capture, photocatalytic proton reduction, CO<sub>2</sub> reduction, and photocatalytic degradation of organic pollutants.<sup>49, 50</sup> Meanwhile, adjustable covalent organic frameworks (COFs) can be used to obtain photocatalytic systems with excellent photocatalytic performance.<sup>51</sup> (i) Modularity, COFs are composed of molecular building blocks, and the basic functions of their photocatalytic process can be regulated by adjusting the molecular structure. (ii) Porosity, the high porosity of COFs provides a high specific surface area, which allows charge to spread rapidly to the surface. (iii) Crystallinity, the periodic structural units of COFs facilitate the transfer of charge and prevent the recombination of charge carriers. (iv) COFs are composed of lightweight elements through covalent bonds, so they have stability, low density, and high gravimetric performance. These mean the potential of COFs in photocatalytic technology research.

Among various nanoporous materials, conjugated microporous polymers (CMPs) are emerging material platform. CMPs have a  $\pi$ -conjugated backbone and a permanent pore structure that distinguish them from unstable porous materials and non-porous conjugated polymers, which were first synthesized by the Cooper's group in 2007.<sup>52</sup> Since their first synthesis, they have been widely studied as an attractive platform for catalytic, energy storage, environmental remediation etc., which can be proved by the number of "Conjugated microporous polymer" keyword index journals that have increased year by year over the past decade (Fig. 1). There are now more than 200 research groups around the world studying CMPs and are on the rise. In 2013, Jiang's group reviewed the design principles, synthesis, and structure of CMPs, and discussed the application of CMPs.<sup>53</sup> They present the properties of CMP materials which are easily regulated by synthesis control such as (i) adjustment of the length and geometric structure of monomers, (ii) use of statistical copolymerization strategies, and (iii) adjustment of reaction conditions.

Compared to traditional inorganic semiconductor materials, CMPs has unique advantages such as low cost, permanent framework and high porosity, high activity and stability, as well as adjustable photoelectric properties, and have been recently under popular research as photocatalysts.<sup>54-58</sup> Few reviews comprehensively and in detail discuss the latest progress of CMPs in the field of photocatalysis, and it is time to fully review the advancements of CMPs in the field of photocatalysis to promote CMP materials and photocatalysis technology further development. Therefore, in this review, we aim to summarize recent progress in using CMPs as a robust platform for artificial photosynthesis and photocatalysis. Firstly, the review introduces the light-harvesting and energy transfer phenomena of CMP materials, and provides guidelines for the rational design of CMPs with excellent photocatalytic performances. Secondly, it extends the photocatalytic applications (e.g. photocatalytic water splitting and CO<sub>2</sub> conversion, organic conversion, and wastewater treatment). Finally, the review presents existing limitations in the field, and proposes the next research prospects. CMP materials have brought new vitality to the field of photocatalysis, and further basic research and application exploration are needed. We hope this review will inspire the interest of readers in these fields of materials science, engineering technology, energy science, and environmental science.

## 2. Basic concept and improvement strategy of CMPs for photocatalysis

### 2.1 Basics of constructing efficient CMP photocatalysts

In nature, the most common photosynthetic unit is a complex network of chlorophyll-proteins. According to the structure classification (Fig. 2),<sup>59</sup> it can be divided into spherical,<sup>60, 61</sup> lamellar,<sup>62, 63</sup> and tubular.<sup>64, 65</sup> In these molecular or supramolecular structures, the absorbed photons produce an excited state on the photosensitive pigment molecules upon receipt of solar energy. This excited state is transported between the phytochrome molecules and eventually transferred to the photoreaction center. In the photoreaction center, the excitation energy is used for charge separation, and active excitation energy is converted into stable chemical energy.

Inspired by natural photosynthesis, scientists have established a variety of artificial photosynthetic systems. CMPs are one of the finest platforms for these systems that combine adjustable conjugated skeleton with permanent microporous structure. Their skeleton acts as a funnel, and the captured energy of the skeleton quickly transfers to the encapsulated guest material. As shown in Fig. 3a, Polyphenylene-based CMPs (PP-CMP) emit blue photoluminescence, which excites energy to migrate across the framework and the charge can be transferred rapidly ( $0.04 \text{ cm}^2 \text{ V}^{-1} \text{ s}^{-1}$ ).<sup>66</sup> The micropores of PP-CMP encapsulate the energy acceptor coumarin 6. The excitation energy on the PP-CMP backbone will be rapidly directed to the coumarin 6 molecule under the synergy of an average of 1.6 phenylene units. The fast, efficient and vector efficiency of energy transfer efficiency of PP-CMP is because of the unique structure. The structure constitutes a spatial confinement for coumarin molecules to make the light-harvesting systems with high efficiency possible. As another example, two fluorescent pyrene-based CMPs (Py-PP and Py-BPP) rendered by the chromophore also have excellent light-harvesting properties because the excitation energy of the mainframe is quickly and efficiently transferred to the encapsulated guest molecules (Fig. 3b).<sup>67</sup> These unique characteristics clearly initiate from their conjugated porous structure of them and demonstrate the usefulness of CMPs in the investigation of the simulated natural light-harvesting supramolecular structure.

The design of artificial photosynthetic systems requires not only light harvesting in a limited nanospace but also the interaction of the various units to achieve efficient energy transfer. CMP materials are constructed from electron donor or electron acceptor unit can be transformed to achieve the blending of highest occupied molecular orbital (HOMO) and lowest unoccupied molecular orbital (LUMO) energy levels, which can effectively improve energy conversion efficiency.<sup>68-70</sup> As shown in Fig. 4a and b, in a ternary system, benzo[1',2'-c:4',5'-c']dithiophene-4,8-dione)); 3,9-bis(2-methylene-(3-(1,1-dicyanomethylene)-indanone))-5,5,11,11-tetrakis(4-hexylphenyl)-dithieno[2,3-d:2',3'-d']-s-indaceno[1,2-b:5,6-b']dithiophene (ITIC) acts as an acceptor, and benzodithiophene-alt-fluorobenzotriazole copolymer (J51) and poly [(2,6-(4,8-bis(5-(2-ethylhexyl)thiophen-2-yl)-benzo[1,2-b:4,5-b']dithiophene))-alt-(5,5-(1',3'-di-2-thienyl-5',7'-bis(2-ethylhexyl) (PBDB-T) are incorporated as donors.<sup>71</sup> This ternary system has good light-harvesting ability and charge transport capability owing to the light capture capabilities of each material and complementary and tandem energy levels between the materials. Fig. 4c confirms that: (i) different monomer doping ratios affect optical characteristics, (ii) appropriate doping

ratio help to reduce joint defects, (iii) adding an appropriate amount of crystal phase improve effectively the surface properties of the thin film in the planar binary system. This strategy suggests that in order to build a type of highly efficient artificial photosynthesis system, in addition to considering the charge separation and migration efficiency of a single CMP surface, we also can design and synthesize binary or multiple CMP systems to achieve efficient solar energy conversion.

## 2.2 Strategies to improve photocatalytic performances for CMPs

As early as the late 1990s and early 2000s, many scientists discovered that conjugated polymers have luminescent and semiconducting properties.<sup>72-75</sup> These polymers can be formed by extending the  $\pi$ -conjugated system.<sup>52, 76-81</sup> As an example, CMP materials were first reported in 2007.<sup>52</sup> Then various CMPs have emerged such as thiophene-containing CMPs,<sup>82</sup> light-emitting CMPs,<sup>83</sup> soluble CMPs,<sup>84</sup> core-shell CMPs,<sup>85</sup> CMP films,<sup>86</sup> comonomer doping CMPs,<sup>87</sup> tetraphenylethylene-interweaving CMPs,<sup>88</sup> and so on (Fig. 5). The photocatalytic performances of these polymers are highly dependent on their surface area, linkage geometry, conjugation degree, and band gap.<sup>89, 90</sup> In recent years, in order to improve the photocatalytic performances of CMP materials, scientists have proposed various improvement strategies.

The molecular structure of CMPs can be regulated by adjusting synthesis methods, reaction conditions, and monomer types, which has been proven to be one of the main strategies to improve their photocatalytic performances. As long ago as 2008, the Cooper's group made continuous fine-tuning of CMPs by changing the length of the monomer for the first time, confirming that the statistical copolymerization method can systematically control the chemical structure and bandgap of CMPs.<sup>77</sup> This provides a useful strategy for the direct synthesis control of the microporous nature of CMP photocatalysts. In 2016, a series of benzothiazole CMPs have highly photocatalytic efficiency with  $2320 \mu\text{mol h}^{-1} \text{g}^{-1}$  for  $\text{H}_2$  evolution reactions (HERs) from water splitting.<sup>91</sup> The results show that the introduction of 3D properties in these linear polymer networks will vastly reduce the photocatalytic efficiency. The higher photocatalytic efficiency of linear polymers than their three-dimensional (3D) crosslinked polymers counterparts may be attributed to their high efficiency of charge transfer, separation, and electron transfer.

The surface area and pore structure of CMP materials can be adjusted easily by using  $\text{SiO}_2$  nanoparticles (NPs) as a template.<sup>92</sup> In this method, a strong electron-withdrawing group is bonded to a weak electron-donating group through a plurality of  $\text{C}_{\text{sp}}-\text{C}_{\text{sp}}$  bonds to form a fully conjugated network with specific electronic properties and pore structures. The Brunauer-Emmett-Teller (BET) surface area of the formed CMPs is double that of a polymer network synthesized without using  $\text{SiO}_2$  NPs as a template. Furthermore, the photocatalytic performances and long-term stability of photocatalysis<sup>93</sup> of them can be improved by changing the monomer distribution and/or introducing comonomers with specific quality. In 2011, a series of CMPs based on pyrene units have been synthesized by statistical copolymerization.<sup>94</sup> These conjugated polymerization networks all have fixed micropores and a high degree of photoluminescence. The photoelectrical properties of pyrene-based CMPs can be fine-tuned by the introduction of luminescent chromophores and by adjusting the distribution of monomers.

Introducing strong electron donors and weak electron acceptors

into the CMP molecular networks and adjusting the ratio of donor to acceptor can effectively enhance the photocatalytic activity of CMPs.<sup>95</sup> A series of donor- $\pi$ -acceptor (D- $\pi$ -A) CMPs with different polymer structures and components were synthesized by using hydrazine, benzothiadiazole, and biphenyl as electron acceptors, electron donors or  $\pi$ -crosslinkers, respectively (Fig. 6).<sup>96</sup> These polymer networks with D- $\pi$ -A structure can expanded the light absorption range, and can effectively separate photo-generated charges, thereby enhanced the photocatalytic performances of these materials.<sup>97, 98</sup> These findings demonstrate the modular nature of CMP materials, and revealing the profound structural effects provide a basic idea for the rational design of CMP photocatalysts. Considering various of electron donors and electron acceptor units, selecting appropriate electron donor and electron acceptor units will build enough D- $\pi$ -A CMP photocatalysts with enhanced photocatalytic properties, which displaying a bright future for photocatalytic applications.

In addition to the molecular structure, the morphology will also affect the photocatalytic performances of CMP materials. CMPs are often synthesized as insoluble and unavailability powders,<sup>99, 100</sup> which are not conducive to popularization. To solve this problem, scientists tried to change the shape of the CMPs, a quintessential example is CMP films. They can be synthesized by an electropolymerization method. In this method, the precursor material undergoes a coupling reaction at the surface of the electrode, and a polymer film is deposited on the surface of the electrode. The thickness of the films is controllable during the synthesis and ranges from nanometers to micrometers. However, previous electropolymerization methods were only studied for N-substituted carbazole units.<sup>86, 101</sup> The synthesized porous organic polymer films have no  $\pi$ -conjugated structure. In 2015, Jiang's group reported for the first time the controllable synthesis of the  $\pi$ -CMP film (thiophene-based CMP film).<sup>102</sup> The porosity, bandgap, conductivity, and prominence of these materials in solar energy conversion systems were explored in this paper. The key to constructing a thiophene-based CMP film is shown in Fig. 7a (blue arrows), that is each thienyl subunit has only one reaction site. Thienyl groups are connected by C-C bonds to form  $\pi$ -conjugate structure under the action of electropolymerization (Fig. 7b). Fig. 7c shows the predicted by computational simulation optimized basic single-hole structure (the inserted is a photo of the films). In these CMP films, the benzotrithiophene (BTT) and the 1,3,5-tri(2-thienyl)-benzene (TTB) play a major role in controlling the growth direction, conductivity, and photoelectric properties of these porous networks. As shown in Fig. 7d, the BTT-CMP films exhibited HOMO and LUMO levels of -5.32 and -3.32 eV, respectively, the TTB-CMP films exhibited HOMO and LUMO levels of -0.54 and -3.19 eV, respectively, and  $\text{C}_{60}$  match the energy levels of these polymer films and can be selected as electron acceptors. Therefore, the  $\text{C}_{60}$  doped into the CMP networks to accelerate charge carrier separation to enhance photoelectric properties (Fig. 7e). This strategy can be extended further to other monomer molecules, which provides guidance for exploring  $\pi$ -CMP films with higher photocatalytic properties.

Stable CMP networks provide excellent support and protection for other active photocatalytic components, which is conducive to form composite photocatalysts with high photocatalytic activity and stability. Many reported photocatalytic CMPs fall into the "naked" photocatalysts. Namely, these CMP photocatalysts are constructed

by conjugated bonding using various bridging ligands having photocatalytic activity without other additional components. In order to facilitate to catalyze valuable but intricate and formidable reactions, multiple functional components can be introduced into the CMP networks through advanced design to form synergistic photocatalysts. The introduction of different functional nanomaterials (e.g. transition metal elements,<sup>103-105</sup> other semiconductor materials,<sup>106, 107</sup> and so on) in CMPs can produce the synergistic interaction between the components to provide enhanced photocatalytic performances.

### 3. CMPs for photocatalytic water splitting

#### 3.1 CMPs for photocatalytic H<sub>2</sub> evolution reaction

The conversion of solar energy into clean chemical energy under the action of artificial photosynthetic systems is a well-received project to promote clean energy instead of fossil energy, which is beneficial to solving global energy and environmental problems. Photocatalytic water splitting is a promising solution among these technologies, which can convert solar energy into valuable hydrogen energy.<sup>108-114</sup> Hydrogen energy is a green, sustainable energy source with three times the gravimetric energy density of gasoline.<sup>114-117</sup> However, photocatalytic hydrogen production strategy still faces many challenges **all around the world**.<sup>118-121</sup> Therefore, it is still necessary to explore more types of materials with the required properties for artificial photosynthetic systems. **In general, the materials used in photocatalytic hydrogen production from water need to meet the following conditions: (i) to be stable against the corrosion of water; (ii) suitable band edge position to meet water redox potential; (iii) suitable band gap to capture more visible photons to generate enough carriers to facilitate the reduction of protons; (iv) suitable energy band structures to facilitate the migration of charge carriers in polymer units; (v) suitable surface chemical reactions.** CMP materials are a novel heterogeneous photocatalysts composed of a conjugated system hopeful for meeting these challenges and have been gained many research advances in recent years.<sup>122-125</sup>

In this section, we briefly discuss CMP materials for photocatalytic H<sub>2</sub> evolution from water splitting with quite a few excellent examples. The quintessential CMPs for photocatalytic H<sub>2</sub> evolution from water splitting and BET surface area, pore-volume, and H<sub>2</sub> evolution related properties of them are summarized in Table 1.<sup>89, 104, 105, 126-138</sup>

As early as 1980, it was reported that porous polymers were used for H<sub>2</sub> evolution, which did not attract much attention. Subsequently, when individuals were found 3D conjugated poly (azomethine) networks to be able to efficiently photocatalysis of H<sub>2</sub> evolution from water splitting in 2010.<sup>139</sup> Various CMPs have been developed to improve the efficiency of H<sub>2</sub> evolution. Cooper's group were prepared a series of polyphenylene-based CMPs (CP-CMP1-15) with tunable bandgap (Fig. 8a).<sup>140</sup> They found that CMPs made of different monomer components have different photophysical characteristics, which are promising photocatalysts for H<sub>2</sub> evolution from water splitting without obvious need for additional cocatalyst. As shown in Fig. 8b and c, a regular redshift in the bandgap is observed as the increase of pyrene monomer content when growing CP-CMP1 to CP-CMP15. The modular chemical strategy used to prepare these polymers is comparable to the synthesis of graphene nanomaterials.<sup>141</sup> This strategy helps to control the electronic

structure and porosity of polymer materials, which will help to advance the design and synthesis of photocatalysts that are comprehensively used for water decomposition.

In a subsequent new study, they prepared a series of extended CMPs such as extended biphenyl CMP (PE-CMP), extended 1,3,5-linked CMP (ME-CMP), extended spirobifluorene CMP (ESP-CMP) to study the important photocatalytic properties (e. g. the geometry of the skeleton, the length of the comonomer, and the degree of planarization of the linker) of these CMPs for photocatalytic produce hydrogen from water splitting.<sup>142</sup> These results and previously reported other findings<sup>78, 99, 143</sup> show that CMP materials have the potential for photocatalytic HERs, but there are differences in effect. Fig. 9a shows the structures of these CMPs. A red-shifted absorption in the solid-phase UV-visible spectrum occurs from CP-CMP1 to PE-CMP (Fig. 9b). They all can act as photocatalysts for hydrogen evolution (Fig. 9c and d). PE-CMP and CP-CMP1 are not ideal for hydrogen production under visible light. The hydrogen production rate of PE-CMP (716  $\mu\text{mol h}^{-1} \text{g}^{-1}$ ) is higher than the CP-CMP1 (164  $\mu\text{mol h}^{-1} \text{g}^{-1}$ ) under UV/visible light (> 295 nm). SP-CMP showed the highest photocatalytic activity and the highest specific surface area. It exhibited the highest hydrogen production rate (1152  $\mu\text{mol h}^{-1} \text{g}^{-1}$ ) under broadband illumination (> 295 nm). However, the general correlation between the porosity of SP-CMP and photocatalytic performance has not been found, which requires further investigation and needs more methods for increasing photocatalytic activity.

The introduction of precious metal nanoparticles in the CMP networks helps to enhance the overall photocatalytic efficiency of these photocatalysts for H<sub>2</sub> evolution from water splitting. As an example, Nagaki reported that the 9,9'-spirobifluorene-based CMP loaded with Pt metal (Pt/COP-3) has a higher rate of hydrogen production than COP-3.<sup>144</sup> COP-3 is an organic polymer having a large specific surface area and a large micropore volume.<sup>145</sup> The HOMO and LUMO levels of COP-3 are enough to oxidize TEOA and reduce H<sup>+</sup>. Direct loading of Pt on COP-3 can be beneficial to increase the transfer of photogenerated electrons and thereby increase the photocatalytic activity to increasing the photocatalytic performances of composite photocatalyst. Recently, A series of Py-based CMPs have been produced by direct C-H arylation coupling reaction for the first proposed.<sup>105</sup> Among them, four-directional pyrene-bithiophene-based CMP (CP1) photocatalytic HERs of 15975  $\mu\text{mol h}^{-1} \text{g}^{-1}$  with AA/DMF/H<sub>2</sub>O as sacrificial agent under visible light without Pt cocatalyst, which are nine times that of one of the highest HERs previously reported organic photocatalysts with ascorbic acid (AA)/MeOH/H<sub>2</sub>O as sacrificial agent (1773.3  $\mu\text{mol h}^{-1} \text{g}^{-1}$ ). It is worth noting that its hydrogen production rate reached an attractive 30810  $\mu\text{mol h}^{-1} \text{g}^{-1}$  after encapsulating 0.5 wt% Pt co-catalyst. Meanwhile, it should also be noted that the presence of DMF is different from the commonly used MeOH sacrificial agents. The non-covalent interaction of hydrogen bonds between DMF and H<sub>2</sub>O contributes to the separation of photogenerated charge carriers. This strategy is a preliminary, simple and attractive new method to enhance the photocatalytic activity by adjusting the reaction matrix, and its mechanism needs further systematic research.

Jiang et al. found that the physicochemical properties (e. g. pore structure, bandgap) of CMPs could be adjusted by changing the type and position of the substituents. As shown in Fig. 10, a series of perylene-containing CMPs (PrCMPs)<sup>146, 147</sup> and a series of

dibenzothiophene dioxide containing CMPs (DBTD-CMPs)<sup>148</sup> have been synthesized by using the Suzuki-Miyaura reaction. The BET surface area of PrPy is higher than PrTPE, which is 1219 m<sup>2</sup> g<sup>-1</sup>, which is attributed to its rigid polymer backbone from planar pyrene units. The physicochemical properties (e. g. pore structure, bandgap) of PrCMPs can be adjusted by changing the type and position of the substituents to obtain optimal photocatalytic properties. The photocatalytic HERs results showed that the increased photocatalytic performances because Pr-CMPs have high conjugated, high specific surface area, a wide range of light absorption, low photoluminescence lifetime and planar structure. The geometry of the linker plays a key role in enhancing the photocatalytic activity of CMP materials. Meanwhile, the crosslinker length has an effect on photocatalytic hydrogen production. The results indicate that short benzene crosslinkers will be more conducive to improving the photocatalytic activity of DBTD-CMPs. This is because the reduction of the length of the cross-linking agent reduces the degree of conjugation and planarization of the CMP molecules, thereby promotes the transport and separation of the light-induced charge carriers. Attractively, adopt a strategy to introducing precious metal catalyst, the DBTD-CMP1 loaded Pt metal showed remarkable high HER (9200  $\mu\text{mol h}^{-1} \text{g}^{-1}$ ) under broad band UV-vis light radiance and high AQY (3.3%) at 400 nm. These studies show that these CMP organic photocatalysts have the prospect for photocatalytic HERs and provide useful guidance for the rational design of these polymers.

In order to accelerate the research and search for excellent performance CMP photocatalysts for H<sub>2</sub> evolution from water splitting, the strategy of combining experiments with theoretical simulations, intelligent robotics, and other new technologies can be considered. One of the pioneers in the field of CMP materials, Cooper and collaborators studied the relationship between the structure of these polymers and their photocatalytic properties for HERs by combining high-throughput calculations and robotic experiments.<sup>149</sup> They use this strategy to systematically build a database of CMP photocatalysts for H<sub>2</sub> evolution from water splitting. In this database, the machine learning model uses four variables (such as electron affinity, ionization potential, bandgap, and polymer particle dispersion in solution) with high correlation to describe the photocatalytic performance of different polymers. Fig. 11a shows the workflow for the synthesis and screening of polymer libraries, and the effective comonomers used in the research to synthesize polymers. In the calculation and test, they considered a total of 6354 copolymers, synthesized and characterized sub-libraries of more than 170 copolymers. Fig. 11b shows the optical properties of 6354 copolymers in the entire polymer library. They predicted and tested these polymers for photocatalytic hydrogen production, and found that all materials have photocatalytic activity for hydrogen production with HERs ranging from 36.8 to 9828  $\mu\text{mol g}^{-1} \text{h}^{-1}$ . Their results show that there is a weak link between the activity of photocatalytic HERs and the single property of the polymer, which supports the opinion that the factors affecting photocatalytic HERs are multifactorial property that relate to many mutually independent factors.

### 3.2 CMPs for photocatalytic O<sub>2</sub> evolution reaction

The other half of the water-splitting reaction, also known as oxygen evolution reactions (OERs), is one of the main challenges for the convenient and widespread production of solar fuel from water. The

formation of photocatalytic molecular oxygen (O<sub>2</sub>) involves a complex multi-electron transfer process, which is an uphill process with a large overpotential and a slow kinetic process.<sup>150-152</sup> Furthermore, it may be useful to study the formation of H<sub>2</sub> and the fixation of CO<sub>2</sub> by the photocatalytic OERs process because the electrons and protons released during the production of O<sub>2</sub> by water splitting have an important role in the formation of H<sub>2</sub> and the fixation of CO<sub>2</sub>.<sup>153</sup> This makes the development of feasible and efficient photocatalytic OERs catalysts get challenging and urgent task. To date, the most common OERs catalysts are noble metal-based materials, which have limited reserves and high cost. An attractive approach is to use the rich elements on the planet to develop low-cost and high-performance catalysts for OERs.

CMPs have adjustable photoelectric and structural properties, which are emerging photocatalysts for OERs. In order to enhance the reactivity of the photocatalytic OERs, poly(1,3,5-triethynylbenzene) (PTEB)<sup>154</sup> and 2D aza-fused CMPs<sup>155</sup> have been used to improve the OERs kinetics. Fig. 12a and b show the synthesis and chemical structure of these CMPs. The energy level of PTEB and aza-CMP film is beneficial to promote water oxidation under the condition of neutral and alkaline (Fig. 12c and d). Remarkably, the bandgap of CMP decreases from 1.65 eV to 1.26 eV as the number of layers increases from 1 to 4. First-principles calculations show that aza-CMP film have the potential to catalyze OERs using visible and near-infrared light. These charge density diagrams of the valence band maximum (VBM) and the conduction band minimum (CBM) (Fig. 12e) further confirm that their highly conjugated structures are conducive to the effective migration of photo-generated electrons to enhance photocatalytic for OERs. The linear sweep voltammograms (Fig. 12f) support one opinion that the nitrogen-doping PTEB (NPTEB) has better catalytic activity than the undoped PTEB. The increase in the catalytic activity of NPTEB may be as follows: (i) an increase in the number of electrochemically active sites; (ii) an increase in pore size; and (iii) an increase in the hydrophilicity of the material, which is important for aqueous reactions. As shown in Fig. 12g, the average OERs rate of aza-CMP film can reach about 1.0  $\mu\text{mol h}^{-1}$  in the presence of electron acceptors under visible light, which exceeds the g-C<sub>3</sub>N<sub>4</sub> photocatalyst (0.12  $\mu\text{mol h}^{-1}$ ). Meanwhile, the results indicate the stability of aza-CMP for photocatalytic OERs that the regenerated aza-CMP film are maintained at the initial value (Fig. 12g). Furthermore, aza-CMP is the first metal-free photocatalyst that has been shown to promote OERs ( $\sim 0.4 \mu\text{mol h}^{-1}$ ) under NIR spectral light ( $\lambda > 800 \text{ nm}$ ), while g-C<sub>3</sub>N<sub>4</sub> is inactive (Fig. 12h). Remarkably, as shown in Fig. 12i, the OERs rate of 3wt% Co(OH)<sub>2</sub>-loaded aza-CMP film increased vastly to 14.3  $\mu\text{mol h}^{-1}$  under visible light, which is four times the original aza-CMP film. This inspires us to develop forms other than amorphous powders of CMP materials.

### 3.3 CMPs for photocatalytic overall water splitting

Photocatalytic water overall splitting can efficiently produce hydrogen and oxygen from water under direct sunlight without the sacrificial agent compared to water splitting half-reacting HERs and OERs.<sup>156-161</sup> Current common photocatalysts for overall water splitting still have disadvantages such as instability, low quantum yield, and unregulated optoelectronic and structural properties.<sup>112, 162-165</sup> Inspired by these challenges of developing high-performance photocatalysts for overall water splitting, scientists have developed simple conjugated polymers with earth-rich elements for low-cost,

efficient and stable photocatalysts for water splitting.<sup>166</sup> However, the challenge is not so easy to succeed. These polymers lose their activity in overall pure water splitting because of the unsuited bandgap, slower separation and migration of photo-generated carriers, and the lack of surface redox sites.<sup>140, 167-170</sup> As an example, although g-C<sub>3</sub>N<sub>4</sub> has been widely used in water splitting half-reacting HERs, it loses activity in the overall pure water splitting reaction.<sup>171-173</sup> In particular, these polymers require a large number of sacrificial agents for photocatalytic H<sub>2</sub> evolution from water splitting, which is not conducive to universal application. Therefore, since the development of these polymer materials science, polymer photocatalysts developed for overall water splitting under visible light in the absence of sacrificial agents have been pursued by scientists in materials science and solar energy conversion engineering.

As an excellent material platform, CMPs can be used for the design of photocatalysts with high catalytic stability and high photocatalytic activity for overall water splitting under visible light. Compared to other conventional photocatalysts, CMPs composed of  $\pi$ -conjugated system, which have excellent chemical stability and thermodynamic stability. Meanwhile, the electron band structure of the benzene ring of the monomer of CMPs has the function of rotation. By changing the dihedral angle between adjacent benzene rings, the structure of CMP materials can be optimized to make them more stable at the energy level. It is well known that the modification of material morphology, such as ultrathin sheet structure, allows the photoexciton to reach the polymer surface quickly, thus inhibiting the recombination of photogenic electron hole pairs and improving the photocatalytic activity of the material.<sup>174, 175</sup> The morphology of CMPs can be adjusted by adjusting the type of reaction, reaction conditions, and monomer types. Furthermore, the band gap of CMPs can be adjusted by band gap engineering so that they have a suitable band gap to absorb visible photons and a suitable band edge potential with reduction and oxidation potentials across water.

For the first time, 1,3-diyne-linked CMP nanosheets (CMPNs) have been synthesized by oxidative coupling reaction and are first applied to photocatalytic overall pure water splitting under visible light.<sup>176</sup> The as-prepared CMPNs with 1,3,5-tris-(4-ethylphenyl)-benzene (TEPB) and 1,3,5-triethynylbenzene (TEB) by oxidative coupling (Fig. 13a) exhibit a sheet-like structure with 6.4 and 630 m<sup>2</sup> g<sup>-1</sup> BET surface area and 1.9 and 3.2 nm average pore size, respectively. Fig. 13b shows that the unique charge distribution characteristics of VBM and CBM of PTEPB and PTEP are conducive to the rapid and efficient transport of photogenerated electrons and holes for water splitting. In the terms of energy, the buckling structure PTEPB is more stable than the flat structure PTEPB. Meanwhile, this work found that CMPNs remained highly catalytic stable after 48 hours of repeat visible light catalytic experiments, suggesting that CMPNs can reduce surface charge accumulation and prevent harmful photochemical degradation. The results of thermogravimetric analysis of two kinds of CMPNs under the action of air show that both PTEPB and PTEB have thermal stability. C 1s XPS spectra and TEM images confirming the CMP structure is highly stable. Furthermore, carbon-carbon triple bonds of 1,3-diyne covalent linkage are Raman-active,<sup>177</sup> which was introduced into the CMP networks can notably reduce the optical gap (from 4.62 to 3.04) to enhance photocatalytic performances for overall water splitting. PTEPB and PTEP catalyze water splitting for the simultaneous generation of H<sub>2</sub> and O<sub>2</sub> under the irradiation of light, and the production ratio is very close to the stoichiometric ratio of H

and O in water molecules. The AQY of PTEPB and PTEP for overall water splitting reaches 7.6%-10.3% under visible light. This even is higher than existing noble metal loaded photocatalysts.<sup>178</sup> This whole reaction process of water splitting by using these polymers is proved by the results of theoretical simulation, which indicated these CMPNs have multiple reaction sites for overall water splitting reaction, which can photocatalyze pure water (pH  $\approx$  7) splitting reaction by a four-electron pathway under visible light (Fig. 13c). This provides a feasible strategy for the development of low-cost and efficient photocatalysts for direct overall water splitting under sunlight without additional input.

#### 4. CMPs for photocatalytic CO<sub>2</sub> reduction reaction

Alongside the photocatalytic water splitting, capturing and converting CO<sub>2</sub> as a part of artificial photosynthesis is also a sustainable solution to energy and environmental issues as well as mitigating global warming.<sup>179</sup> Artificial supramolecular structures to stimulate artificial photosynthesis for converting CO<sub>2</sub> into sustainable fuels by using solar energy is a promising strategy, yet a formidable challenge. Their advantages have mild operating conditions, abundant and cheap raw materials, and high-value products. Meanwhile, their challenges now are that few materials can overcome the high bond energy ( $\sim$ 750 kJ mol<sup>-1</sup>) of CO<sub>2</sub> and efficiently convert CO<sub>2</sub>.<sup>180</sup> Previous research reports briefly described the basic concepts and principles of photocatalytic reduction of CO<sub>2</sub> under sunlight, and emphasizing the shortcomings of low light energy conversion efficiency and poor selectivity of existing photocatalytic materials.<sup>119, 181-184</sup> They are suggested to design a highly active catalytic system from the four opposite sides, such as the adsorption of reactants, the separation and transfer of charges, the collection of light, and the activation of CO<sub>2</sub>. These available strategies include:<sup>184</sup> (i) effective adjustment of the band gap and band position of material molecules; (ii) material nano-crystallization for rapid separation and transfer of photo-generated electron pairs; (iii) improvement of the surface properties of materials for CO<sub>2</sub> adsorption and activation; (iv) the formation of the channels on the structure, which increasing the surface area of photocatalysts for increasing the adsorption of reactants and providing more surface-active sites; (v) exposure facet engineering for adjust the electronic band structure; (vi) development of composite photocatalyst for effective reduction of the activation barrier of CO<sub>2</sub>; (vii) development of Z-scheme photocatalytic systems for promoting surface chemical reaction and inhibiting reverse reaction of redox reaction. Nowadays, CMPs as emerging and promising photocatalytic materials get the attention of the public.<sup>185</sup> Combining some CO<sub>2</sub> activation methods<sup>186-188</sup> with adjustable properties of CMPs are expected to provide a new solution for photocatalytic CO<sub>2</sub> reduction. Table 2 is summarized the state-of-the-art development of CMPs for photocatalytic CO<sub>2</sub> reduction, including their molecular structure, photoelectric properties, pore properties, photocatalytic properties, and so on.<sup>189-192</sup>

Porphyry tetracyclic compounds, as important compounds in the process of life evolution, are widely used in artificial light energy conversion systems.<sup>193-195</sup> Among them, metalloporphyrin derivatives can be used for photocatalytic CO<sub>2</sub> reduction.<sup>196-199</sup> Moreover, 2D polymers expose more active sites, which has higher photocatalytic efficiency.<sup>200-202</sup> Taking into account the advantages of 2D CMPs, the photocatalytic activity of metalloporphyrin derivatives for CO<sub>2</sub>

reduction, and the dye-sensitizing effect of thiophenes, the metal-modified 2D metalloporphyrin CMPs can be used to improve the ability of photocatalytic reduction of CO<sub>2</sub>. These CMPs constituted by introducing a series of metal atoms (Fe, Mg, etc.) into a novel thiophene-linked porphyrin polymer center, which can improve the electronic properties of these polymers, thereby promoting the CO<sub>2</sub> reducing ability.<sup>203</sup> The research presented iron-modified CMPs have the highest CO<sub>2</sub> reduction capacity, which may be attributed to the unique semi-metallic properties and band structure. The intermediates involved in CO<sub>2</sub> reduction are shown in Fig. 14a, and the reaction steps and activation energy (E<sub>a</sub>) of various species involved in the CO<sub>2</sub> reduction process are shown in Fig. 14b. In the carboxyl pathway, CO<sub>2</sub> is finally reduced to CH<sub>4</sub>, and the by-product is HCOOH, which is the preferred thermodynamics reduction process. CH<sub>4</sub> is easily removed from the Fe-CMP substrate to vacate the reactive sites for other CO<sub>2</sub> molecules, facilitating the continued reduction of the reduction reaction. This outstanding research provides a new idea for the structural design of 2D metalloporphyrin CMP materials. Meanwhile, it provides a new path for photocatalytic reduction of CO<sub>2</sub>.

A triazine-based CMP molecular networks can activate and reduce CO<sub>2</sub> in the visible light because the substituent group (thiophene) on the triazine-based CMP backbone can promote charge separation.<sup>190</sup> These CMPs are synthesized by coupling various electron-donor and -acceptor monomers (Fig. 15a). The HOMO levels and the LUMO levels of these polymers can be adjusted by introducing different monomers (Fig. 15b), and the efficiency of photocatalytic CO<sub>2</sub> reduction can be improved by introducing different electron donor and electron acceptor groups. Among them, CMP-BT has the highest photocatalytic activity (CO/H<sub>2</sub>: 1213.33 μmol h<sup>-1</sup>g<sup>-1</sup>/273.33 μmol h<sup>-1</sup>g<sup>-1</sup>) and stability (recycle 6 times) (Fig. 15c and d), and the results show that the selectivity of CMP-BT reached 81.6%, and the maximum AQY (at 405 nm) reached 1.75% (Fig. 15e).

As a robust platform, CMPs can be used to design photocatalysts with specific properties by changing the organic monomers and synthesis methods. For example, in order to control the selectivity of photocatalysts, researchers could consider using CO<sub>2</sub>-philic monomer to construct CMP networks, which is helpful for efficient capture and further highly selective conversion of CO<sub>2</sub>. Recently, using this strategy, PEosinY-1 with high BET surface area (620 m<sup>2</sup> g<sup>-1</sup>) has been synthesized by coupling of Eosin-Y with 1,4-dithynylbenzene, which can efficiently promote photoreduction for conversion of CO<sub>2</sub> to CO (yield: 33 mmol g<sup>-1</sup> h<sup>-1</sup>) with highest selectivity of 92% (Table 2) under visible light without any photosensitizer or sacrificial reagent.<sup>191</sup> Fig. 16 shows the possible mechanism for photocatalytic CO<sub>2</sub> reduction by using PEosinY-1. These outstanding contributions provide new horizons for the design and assembly of polymer-based photocatalysts for solar energy conversion with high performance.

## 5. CMPs for photocatalytic organic conversion

Solar-driven organic conversion is a powerful tool for the synthesis of many important compounds. Photoactive transition metals (as Ru, Ir, etc.) are one of the first materials for light-driven organic conversion. These materials have some inherent disadvantages such as high cost, low earth reserves, and lack of catalytic stability.<sup>204-210</sup> Therefore, the development of recyclable and metal-free high-efficiency heterogeneous catalysts for organic conversion remains a great

challenge. In recent years, CMPs as a new class of recyclable metal-free photocatalysts have attracted great attention in photocatalytic organic conversion owing to their high BET surface areas, high stability and adjustable functional.<sup>211-215</sup> Scientists have explored the photocatalytic performances of CMPs in organic conversion including α-alkylation of aldehydes, oxidative coupling of amine, hydroxylation of arylboronic acid, aza-Henry reaction, and Stille-type coupling reactions (Table 3).<sup>214, 216-225</sup>

Each monomer of CMP materials connected by a conjugated bond, and they synthesized by using silica as a template with high reaction conversion rates in organic conversion, but the efficiency and reaction rate are not high.<sup>92</sup> To solve this problem, the rigid structure of metallophthalocyanine-based CMP (MPC-CMP) can be considered.<sup>226</sup> The rigid porous structure of MPC-CMP can effectively prevent the polymerization of MPC units, thereby increasing the chance of contact between the reactive sites and the reaction substrate. Moreover, BODIPY (4,4-difluoro-4-bora-3a,4a-diazasindacene) dye with high quantum yields and high photocatalytic stability<sup>227-230</sup> can be introduced in CMP networks is beneficial to synthesis the BODIPY-based CMP (CMPBDP) with good performance for organic conversion. There are two main methods for synthesizing CMPBDP: (i) palladium metal-catalytic Suzuki-Miyaura coupling reaction, and (ii) metal-free catalytic post-synthesis conversion method.<sup>231</sup> The BET surface area of the synthesized CMPBDP reached 484–769 m<sup>2</sup> g<sup>-1</sup>. It has high stability, high surface area and high efficiency heterogeneous photocatalytic activity in organic conversion, and it as photocatalyst for oxidation of thioanisole is four times faster than the corresponding soluble photocatalyst, and it can be recycled multiple times under visible light irradiation.<sup>232</sup> These findings indicate that these CMP networks are excellent photocatalytic properties for organic conversion.

As an excellent platform, CMP materials not only have its own photocatalytic activity but also provides stable support for various photocatalytic materials for organic photocatalysis. The interface between CMPs and Pd NPs with heterojunction effect is beneficial for enhancing photocatalytic activity to the Suzuki coupling reaction.<sup>233</sup> The experimental results show that Pd@CMP has the right level of energy, uniformly dispersed Pd NPs (Fig. 17a), unique optical properties (Fig. 17b and c), and excellent photocatalytic performances (yield: 98%, under visible light). The electrons generated by the semiconductive polymer B-BO<sub>3</sub> are transferred to the active center of Pd NPs and attack the C-I bond of iodobenzene in the reaction, which promotes the completion of the reaction under visible light irradiation (Fig. 17e). Meanwhile, Pd@B-BO<sub>3</sub> is easily separated from the reaction substrate and recycled, which does not cause a big loss of activity in further reactions. The same strategy also can be applied to other classic C-C coupling reactions such as Heck reactions, Sonogashira reactions, and so on.

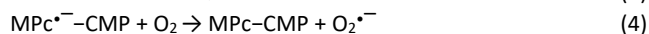
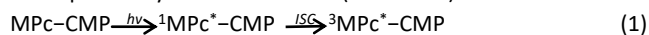
Few studies have so far used direct natural light as a source of photocatalytic technology. Light sources have always been the main part of the long-term cost of photocatalytic technology. To reduce the cost of photocatalytic organic conversion, it is necessary to explore the photocatalytic organic conversion of direct natural light. The CMP-CSU6 derived from 1,3,5-tri(9H-carbazol-9-yl)benzene synthesized by using the FeCl<sub>3</sub>-mediated Friedel-Crafts reaction showed a high BET surface area (1022 m<sup>2</sup> g<sup>-1</sup>) and adjustable band gap range.<sup>234</sup> It can effectively photocatalyze the conversion of hydrazine at room temperature under natural light, and can retain its

original photocatalytic activity after at least five cycles. Furthermore, a metal-free truxene-based CMP (Tx-CMP) has a narrow band gap (2.6 eV) with the ability to catalyze the oxidation of amines under direct sunlight.<sup>235</sup> Tx-CMP with high BET surface area and flake structures are synthesized by introducing a Tx molecule in CMPs. Their proper band gap is favorable for promoting photocatalytic oxidation reaction. Compared with TiO<sub>2</sub> and SG-CN, Tx-CMP photocatalyst has higher catalytic activity (conversion > 99%) for catalyzing the oxidative isotope coupling reaction of amines owing to their high BET surface area and suitable band gap. It should be noted which is the high catalytic activity and selectivity of Tx-CMP driven by sunlight can be maintained for at least five cycles. The carriers, holes, and electrons generated after Tx-CMP absorb light is used to drive the reaction (Fig. 18). The latest research is still going on, expecting photocatalytic technology to bring more "light" to our lives.

## 6. CMPs for photocatalytic degradation of organic dyes

With the progress of industrialization, the discharge of a large number of organic pollutants into the environment poses a great threat to the ecological environment.<sup>236-240</sup> Among them, organic dyes are one of the most common contaminants, and they are widely concerned because they are non-biodegradable and carcinogenicity. In order to protect the safety of the ecological environment, it is urgent to develop an efficient, low-energy and sustainable technology to remove organic dyes from water. For this purpose, emerging materials are used in the study of photocatalytic degradation of organic dyes.<sup>241-244</sup> Among them, CMPs are one of the most promising photocatalytic materials. These CMP materials are combining high porosity with good solution dispersion can facilitate the uniform contact of the heterogeneous materials with contaminants to increase the photocatalytic degradation activity. Meanwhile, they can joint different electron donor and acceptor groups, changing the structure (such as microspheres, nanorods, and nanofilms) to facilitate charge transfer and increase redox sites to enhance degradation efficiency. They are an ideal photocatalysts with high activity, high stability, and recyclability for photocatalytic degradation of organic dyes (Table 4).<sup>245-254</sup>

The main active substances that promote degradation is singlet oxygen (<sup>1</sup>O<sub>2</sub>), superoxide radical (<sup>•</sup>O<sub>2</sub><sup>-</sup>), photogenerated hole (h<sup>+</sup>) and HO<sup>•</sup> that produced in the photocatalytic reactions. According to preliminary work prediction, the mechanism of photocatalytic degradation pathway of rhodamine B (RhB) by using metallophthalocyanine-based CMP (MPC-CMP) is as follows:<sup>255-258</sup>



(ISC: intersystem crossing).

In the above formula, MPC-CMP is converted to an intermediate singlet state by photoexcitation, and then converted to a triplet state by an ISC transition [eqn. (1)]. <sup>3</sup>MPC<sup>\*</sup>-CMP reacts with molecular oxygen to convert to free radical cation form of MPC-CMP and O<sub>2</sub><sup>•-</sup> [eqn. (2)]. Meanwhile, <sup>3</sup>MPC<sup>\*</sup>-CMP oxidizes RhB to a free radical cationic form and produces a free radical anionic form of MPC-CMP [eqn. (3)]. The free radical anion of MPC-CMP reacts with oxygen [eqn. (4)], and O<sub>2</sub><sup>•-</sup> is protonated to produce HO<sub>2</sub><sup>•</sup> [eqn. (5)]. Meanwhile, OH<sup>•</sup> radicals are formed [eqn. (6)], and they also can be generated when hydrogen peroxide is excited by light [eqn. (7)]. These free radicals from the above reactions are the main active substances to degrade organic dyes [eqn. (8) and (9)].

Highly dispersed nanostructured CMPs (CMP NPs) exhibit high photocatalytic activity for the degradation of organic dyes under the illumination of household lamps.<sup>259</sup> Various monomers used for different CMP NPs as well as their design principle and the synthesis route are shown in Fig. 19a. Scanning electron microscope (SEM) and transmission electron microscope (TEM) images of CMP NPs are shown in Fig. 19b. The morphology of synthetic CMPs is related to their monomers such as containing triple bonds, which have a more rigid and expanded network backbone than CMPs containing single bonds. These CMPs are excited by light to generate photo-generated electron-hole pairs, and then they are separated and migrate to the valence band (VB) and conduction band (CB) as redox sites for redox reactions. The results show that they can efficiently degrade RhB in water (degradation: 80%, 25 min) because the high dispersion of CMP NPs have many surface-active sites (Fig. 19c). <sup>1</sup>O<sub>2</sub> is the main active substance for photocatalytic degradation of RhB proved by Fig. 19d. Meanwhile, these photocatalysts can be recycled many times without inactivation, which provides an economically viable solution for photocatalytic degradation of organic dyes.

Using the same composition strategy, a new Anderson-type polyoxometalate (POM) built-in CMPs constructed by two tetrabromo-bifunctionalized Anderson-type POMs: (TBA)<sub>3</sub>{MnMo<sub>6</sub>O<sub>18</sub>[(OCH<sub>2</sub>)<sub>3</sub>CNH(C<sub>7</sub>H<sub>3</sub>Br<sub>2</sub>O)]<sub>2</sub>} (1) and (TBA)<sub>3</sub>{MnMo<sub>6</sub>O<sub>18</sub>[(OCH<sub>2</sub>)<sub>3</sub>CNH(C<sub>5</sub>HBr<sub>2</sub>OS)]<sub>2</sub>} (2) are obtained for the first time (Fig. 20a).<sup>260</sup> SEM and TEM images demonstrate the morphology of these two CMP NPs (Fig. 20b). These two POM-based CMP NPs have a diameter of about 30 nm and with a homogeneous distribution. They show a broad absorption band for efficient photocatalytic degradation of organic dyes. RhB degradation and methylene blue (MB) degradation both are > 99% in presence of these CMP photocatalysts under 1 h of visible light source irradiation at room temperature (Fig. 20c and b), and <sup>1</sup>O<sub>2</sub> and H<sub>2</sub>O<sub>2</sub> are main active substance for the degradation of organic dyes. Then Recycling experiments proved these photocatalysts can be cycled in the photocatalytic degradation of MB at least five times without reducing catalytic activity (Fig. 20e). Improving the stability and increasing the number of reusable times of photocatalysis are beneficial to reduce the cost of photocatalysis technologies.

The stability and recoverability of photocatalysts are critical to their availability in various photocatalytic applications include photocatalytic degradation of organic dyes. However, a common problem is the catalytic activity of organic dyes makes them easy to be dissolved and dissociated in the reaction medium and prone to photobleaching, which hinders the recovery and long-term use of photocatalysts. Nanostructures have a high surface-to-volume ratio and porous materials have a larger surface area, which is conducive

to solving this problem. With high surface-to-volume ratio and large surface area, CMPs are a powerful platform for the design of stable and easily recycled new metal-free heterogeneous photocatalysts. As two quintessential examples, the degradation rates of organic dyes degraded by P-FL-BT-3<sup>245</sup> or Py-BF-CMP<sup>249</sup> in water under 1 h of visible light irradiation is higher than 90% and can be reused for 10 times without inactivate (Table 4).

Recently, a novel phthalocyanine-based CMPs ( $\alpha$ -ZnPc-CMP and  $\beta$ -ZnPc-CMP) with a rigid linker are copolymerized by using zinc phthalocyanine (ZnPc) and 4,6-diaminoresorcinol dihydrochloride (DADHC) for promoting the cycle times of photocatalysts in the degradation of organic dyes.<sup>261</sup> These CMPs have a highly ordered skeleton arrangement and a two-dimensional (2D) open channel structure, which is advantageous for solving the problem of ZnPc aggregation to avoid secondary pollution and improves the recyclability of the photocatalysts. Treat insoluble  $\alpha$ -ZnPc-CMP and  $\beta$ -ZnPc-CMP with different solvents such as water, various organic solvents, strong hydrochloric acid and high concentration of sodium hydroxide 24 h for test the stability of these CMP photocatalysts. The results prove that they have completed these challenges, and are stable in different solvents, as well as can be reused for photocatalytic reactions after simple filtration.

CMPs and their composite materials provide a path worthy of further exploration for the application in removing organic dyes in water. A series of metal phthalocyanine-based CMPs (MPC-CMPs) materials<sup>258</sup> and benzobisoxazole-linked porphyrin-based CMPs (BBO-Por-CMPs and BBO-MPor-CMPs)<sup>262</sup> were first synthesized for photocatalytic degradation of high concentrations of organic dyes, which have a fully conjugated system and are a class of non-toxic, stable photocatalysts. The specific surface area and backbone structure of CMPs are key factors affecting photocatalytic activity for the degradation of organic dyes because a higher specific surface area can increase the amount of adsorption of contaminants. Meanwhile, the linear polymer exhibits a narrower bandgap and higher charge transfer efficiency because they have a better extended conjugated system.<sup>263</sup> Furthermore, composite photocatalysts composed of TiO<sub>2</sub> and CMPs have enhanced photocatalytic ability to degrade organic dyes.<sup>264</sup> The photocatalytic degradation rate of TrCMP-TiO<sub>2</sub> composite prepared by the hydrothermal method is several times higher than that of TiO<sub>2</sub> material alone and other similar photocatalysts,<sup>265, 266</sup> which can remove 96% MB under 1 h of visible light irradiation.

## 7. CMPs for photocatalytic sterilization and disinfection

Photocatalytic technologies are being actively researched in the fields of environment and medicine.<sup>267-269</sup> A large number of pollutants produced by human activities and the harmful bacteria occurring from nature pose a great threat to human health and the ecological environment.<sup>270</sup> Especially the emergence of resistant bacteria is one of the main challenges facing modern public health.<sup>271-274</sup> As an antibacterial material, CMPs can produce large amounts of singlet oxygen (<sup>1</sup>O<sub>2</sub>) under visible light illumination in antibacterial photodynamic therapy,<sup>81, 92, 259, 275</sup> which can inactivate bacteria (Fig. 21).<sup>226, 276, 277</sup> These materials have two forms: (i) evenly dispersed in water, which can inactivate bacteria in water under

visible light, and (ii) hydrogel nanofiber membranes, which inhibit bacterial growth under visible light conditions and to provide continuous protection for the wound.

A high-efficiency photosensitive CMP NPs synthesized by combining an electron-withdrawing group to a network structure with electron supply properties by using the Suzuki-Miyaura reaction are used as a class of highly effective photosensitizing antibacterial agents (Fig. 22a).<sup>278</sup> They are highly dispersed in aqueous solution and produce <sup>1</sup>O<sub>2</sub> under visible light irradiation for effectively kill bacteria in water (Fig. 22b). Furthermore, a hydantoin group is introduced into a CMP network (CMPH) to prepare a novel CMP antibacterial agent.<sup>279</sup> The antibacterial agent can be fabricated not only into a single piece of nanoporous foam but also on other inert materials to produce a low-cost bactericidal material for medical supplies. In a simple one-pot reaction vessel, CMPH alters the permeability of the bacterial cell membrane, which causes bacteria (such as *E. coli*, *Staphylococcus aureus*, etc.) inactivation. These findings open a versatile door to the design and manufacture of CMP antimicrobial materials. A wide variety of photosensitive antibacterial agents can be produced by introducing different antibacterial substituents into the CMP networks. Interestingly, a new type of hydrogel nanofiber membrane has recently emerged that exhibits visible-light-driven disinfection. The CMP NPs are embedded in poly(ethylene glycol) hydrogel nanofibers by a colloid-electrospinning process and crosslinked into nanofiber films under glutaraldehyde/HCl vapor conditions.<sup>280</sup> This synthetic strategy allows for a flexible combination of different CMP NPs with different nanofiber support materials. These nanofiber films exhibit high biocompatibility and they will be a promising candidate for a new generation of wound dressings given the photoactivity.

## 8. Conclusions and perspectives

In recent years, CMPs have been extensively studied and developed for photocatalysis. This review mentions CMPs as a promising platform for photocatalytic applications covering water splitting, CO<sub>2</sub> reduction, organic conversion, and degradation of organic dyes, as well as sterilization and disinfection. Although these materials have proven to be excellent promising photocatalysts, more efforts are still needed to compete with more traditional and mature photocatalysts, which needs to give great attention in the following aspects in the future.

### 8.1 Design and synthesis

Most of the synthetic methods of CMP photocatalysts involve noble metal-catalyzed C-C cross-coupling reactions. Industrial and commercial applications of CMPs have been limited because they have some disadvantages such as high cost, harsh reaction conditions, and limited metal reserves. Meanwhile, trace metals remaining on the surface of the CMPs are difficult to remove by purification. The effect of residual trace metals on the photocatalytic performances of CMPs needs to be clarified.

The wide variety of synthetic conditions are available to polymerize not only various functional group monomers but it is also promising to find suitable synthetic strategies for introducing photocatalytically active components into the CMP networks for more challenging reactions. There are many CMP materials on the category, but not every CMP materials have photocatalytic activity. Encapsulation of a

metal dipyrindine complex or a noble metal nanoparticle with a plasma effect in a CMP channel is an attractive strategy for the preparation of robust composite photocatalytic materials.

However, this method is also accompanied by some problems such as the encapsulated functional components are easy to leach from the porous framework, which resulting in catalyst deactivation and environmental pollution. It is solved will help to improve the catalytic activity and service life of the composite photocatalysts and improve its economic viability as well as bring a wider range of industrial and commercial applications. Furthermore, an important point is necessary to find inexpensive and scalable synthetic methods to form CMPs. We developed CMPs for photocatalysis with the aim of finding cleaner production methods. There is not enough to improve the performance of the materials, it also is important to pour attention into the fact that the material itself needs to be consistent with the principles of sustainable development.

### 8.2 Morphology, molecular structure, and porosity

CMPs are rigid and distorted organic molecules linked by covalent bonds. Strong covalent bond connections impede the formation of reversible bonds, which creates an inherent disadvantage of CMP materials that they are completely amorphous. The amorphous powder morphology of CMPs is detrimental to their photocatalytic applications. In recent years, the morphology of CMPs is oriented towards diversity for further development, such as the advancement of other morphologies (e.g. nanofilm, nanoparticle, nanorod, and nanotube). These will provide more possibilities for applications of CMPs. Meanwhile, in order to design more excellent CMP photocatalysts, more efforts are needed in the following directions: (i) further studies of exciton migration and charge carrier migration of CMPs is needed, which improves charge transfer and conductivity of these polymers, thereby improving their photocatalytic performances; (ii) the molecular structure and photocatalytic performances of CMP materials need to be clarified systematically; (iii) further research on synthesizing low bandgap CMPs is required.

Space-efficient packing of polymer chains is effectively carried within these structures forming a large free volume, such structures being referred to as microporous structures. CMPs provide a powerful means of controlling microporous structures, pore environment and function. The surface area of these microporous materials usually exceeds 1000 m<sup>2</sup> g<sup>-1</sup>. However, the BET surface area and pore volume of CMPs still need to be improved to enhance photocatalytic performances. The mainly research directions as following: (i) improvement of polymerization and crosslinking of CMPs, which can help to increase the BET surface area of these materials; (ii) reduction of the flexibility of the monomer link, which can reduce the length of the pillars between the monomer molecules, which requires the use of short, rigid comonomers; (iii) dimension control of CMPs, which help to increase the BET surface area such as 3D structures of CMPs are generally higher than the surface area of 2D CMPs.

### 8.3 Solar conversion efficiency

The spread of photocatalytic technologies needs to improve the efficiency of solar energy to reduce costs. The energy consumption of artificial light source is one of the main factors that the cost of photocatalysis does not decrease. Therefore, it is of long-term significance to explore the photocatalytic process of using natural sunlight. In order to efficiently use of direct sunlight to reduce the

cost of photocatalysis, the researches has two trends: (i) one is building an efficient light-harvesting system at the molecular level to absorb efficiently solar energy that radiates onto the surfaces of CMPs; (ii) the other is designing a good external light absorption system, also known as optical trap, to allow more sunlight can irradiate the surface of CMPs.

### 8.4 Catalytic stability

Stability is an important and universal challenge facing polymer porous materials in the future. Synthetic polymer-based porous materials require mechanical stability, and most applications of the porous solids require stability at least in the air. For thermal stability, these new materials have sufficient thermal stability in the process of heterogeneous catalysis at lower temperatures. For other applications, such as carbon dioxide capture, require these materials to be stable in wet, acidic conditions.<sup>281</sup> In term of photocatalysts, these materials are required to maintain long-term stability under intense light irradiation.<sup>140</sup> CMPs are generally chemically stable, however, we believe that further studies should be investigated on their stability before they can be used commercially. For example, the long-term photochemical stability of CMPs deserves to be discussed in more detail. Especially in the aspect of synthetic organic conversion, the use of long-term stable CMPs as heterogeneous photocatalysts helps to reduce the use of expensive metals and simplify the recovery and reuse of catalysts.

### 8.5 Application prospects

In general, these polymer-based porous materials are synthesized from monomers with hydrophobic groups and/or bio-repulsive groups. Hydrophilicity and biocompatibility issues need to be considered when attempting to compare these materials with enzyme systems and other commercial catalysts in applications including biosensors, electrocatalytic water splitting, and energy storage. The simple use of monomers with hydrophilic and/or biocompatible groups in synthesis process of the polymers could destroy the overall binding of the polymers and affect their photoelectric properties. The post-synthetic modification<sup>282, 283</sup> is expected to be a solution to this problem. Furthermore, in the field of photoelectric catalysis, the energy level matching of the highest occupied molecular orbital (HOMOs) and lowest unoccupied molecular orbitals (LUMOs) between the components of the device facilitates the maximum energy conversion efficiency. Designing a reliable and clear method or technique to help adjust the HOMO and LUMO levels of CMPs could lead to a major advance in these materials.

CMPs are not crystalline, so they have more flexibility in design than crystalline COFs, and are more likely to design multi-component, multi-functional catalysts. In order for these materials to have greater industrial application, it is necessary to optimize multiple functions, such as pore structure, surface area, stability, adsorption kinetics, and workability. As an excellent material platform, CMPs has thousands of monomers, and a single solution cannot solve all the problems. Therefore, it can be challenging to choose the right monomer for a particular application. Theoretical calculations and artificial intelligence (AI) could provide additional insights in determining the best material structure for specific applications.

As CMPs have many inherent advantages such as monomer diversity, adjustable molecular structures and morphologies, and stable conductive properties, there are potentials in developing these

polymers for photocatalytic applications. Combining the state-of-the-art of material science, theoretical calculations, and AI, the key innovations of CMPs for photocatalytic technologies will be a blowout. We hope this review can provide a useful guide for future developments in the materials science and photocatalytic technology to solve challenging environmental and energy issues.

## Author contributions

S.H.L., Z.T.Z., G.M.Z., Z.F.L., and R.X. conceived the work, analyzed the cited references and wrote the paper. All authors discussed the details of the article and commented on the manuscript.

## Conflicts of interest

There are no conflicts of interest to declare.

## Acknowledgments

The study was financially supported by the Program for Changjiang Scholars and Innovative Research Team in University (IRT-13R17), the National Natural Science Foundation of China (51521006, 51679085, 51579096, 51378192, 51039001, 51378190, 51508177), the Fundamental Research Funds for the Central Universities of China (531107050930, 531107051205), the Funds of Hunan Science and Technology Innovation Project (2018RS3115), the Key Research and Development Project of Hunan Province of China (2017SK2241) and the Three Gorges Follow-up Research Project (2017HXXY-05).

## Notes and references

- J. I. Lewis, D. G. Fridley, L. K. Price, H. Lu and J. P. Romankiewicz, *Science*, 2015, **350**, 1034-1036.
- D. Shindell and C. J. Smith, *Nature*, 2019, **573**, 408-411.
- D. Tong, Q. Zhang, Y. Zheng, K. Caldeira, C. Shearer, Z. Hong, H. Qin and S. J. Davis, *Nature*, 2019, **572**, 373-377.
- Y. Wang, H. Suzuki, J. Xie, O. Tomita, D. J. Martin, M. Higashi, D. Kong, R. Abe and J. Tang, *Chem. Rev.*, 2018, **118**, 5201-5241.
- J. J. Zhang, H. Wang, X. Z. Yuan, G. M. Zeng, W. G. Tu and S. B. Wang, *J. Photochem. Photobiol. C*, 2019, **7**, 1-26.
- J. Gong, C. Li and M. R. Wasielewski, *Chem. Soc. Rev.*, 2019, **48**, 1862-1864.
- D. Gust and T. A. Moore, *Science*, 1989, **244**, 35-41.
- F. Wen and C. Li, *Acc. Chem. Res.*, 2013, **46**, 2355-2364.
- M. D. Kärkäs, O. Verho, E. V. Johnston and B. Åkermark, *Chem. Rev.*, 2014, **114**, 11863-12001.
- M.-Q. Yang, N. Zhang, M. Pagliaro and Y.-J. Xu, *Chem. Soc. Rev.*, 2014, **43**, 8240-8254.
- L. Sun, *Science*, 2015, **348**, 635.
- M. Rudolf, S. V. Kirner and D. M. Guldi, *Chem. Soc. Rev.*, 2016, **45**, 612-630.
- B. Zhang and L. Sun, *Chem. Soc. Rev.*, 2019, **48**, 2216-2264.
- A. Fujishima and K. Honda, *Nature*, 1972, **238**, 37-38.
- A. Fujishima, X. T. Zhang and D. A. Tryk, *Surf. Sci. Rep.*, 2008, **63**, 515-582.
- T. P. Yoon, M. A. Ischay and J. Du, *Nat. Chem.*, 2010, **2**, 527-532.
- W. Zhen, J. Ma and G. Lu, *Appl. Catal. B*, 2016, **190**, 12-25.
- X. Hao, Z. Jin, H. Yang, G. Lu and Y. Bi, *Appl. Catal. B*, 2017, **210**, 45-56.
- H. Wang, X. Liu, S. Wang and L. Li, *Appl. Catal. B*, 2018, **222**, 209-218.
- D. Huang, S. Chen, G. Zeng, X. Gong, C. Zhou, M. Cheng, W. Xue, X. Yan and J. Li, *Coord. Chem. Rev.*, 2019, **385**, 44-80.
- S. Chen, D. Huang, G. Zeng, X. Gong, W. Xue, J. Li, Y. Yang, C. Zhou, Z. Li, X. Yan, T. Li and Q. Zhang, *Chem. Eng. J.*, 2019, **370**, 1087-1100.
- S. Luo, Z. Zeng, G. Zeng, Z. Liu, R. Xiao, M. Chen, L. Tang, W. Tang, C. Lai, M. Cheng, B. Shao, Q. Liang, H. Wang and D. Jiang, *ACS Appl. Mater. Inter.*, 2019, **11**, 32579-32598.
- M. Neumann, S. Fuldner, B. König and K. Zeitler, *Angew. Chem. Int. Ed.*, 2011, **50**, 951-954.
- M. L. Marin, L. Santos-Juanes, A. Arques, A. M. Amat and M. A. Miranda, *Chem. Rev.*, 2012, **112**, 1710-1750.
- X. Huang, X. Qi, F. Boey and H. Zhang, *Chem. Soc. Rev.*, 2012, **41**, 666-686.
- R. Lin, L. Shen, Z. Ren, W. Wu, Y. Tan, H. Fu, J. Zhang and L. Wu, *Chem. Commun.*, 2014, **50**, 8533-8535.
- F. Chen, Q. Yang, Y. Zhong, H. An, J. Zhao, T. Xie, Q. Xu, X. Li, D. Wang and G. Zeng, *Water Res.*, 2016, **101**, 555-563.
- L. Zhang, C. G. Niu, C. Liang, X. J. Wen, D. W. Huang, H. Guo, X. F. Zhao and G. M. Zeng, *Chem. Eng. J.*, 2018, **352**, 863-875.
- S. Cao, J. Low, J. Yu and M. Jaroniec, *Adv. Mater.*, 2015, **27**, 2150-2176.
- Y. Yang, C. Zhang, J. Li, Huan, G. M. Zeng, J. H. Huang, C. Lai, C. Y. Zhou, W. J. Wang, H. Guo, W. J. Xue, R. Deng, M. Cheng and W. P. Xiong, *Appl. Catal. B*, 2019, **245**, 87-99.
- D. L. Huang, Z. H. Li, G. M. Zeng, C. Y. Zhou, W. J. Xue, X. M. Gong, X. L. Yan, S. Chen, W. J. Wang and M. Cheng, *Appl. Catal. B*, 2019, **245**, 153-173.
- L. Huang, H. Hu, Y. Shi, G. Zeng, W. Cheng, H. Yu, Y. Gu, L. Shi and K. Yi, *J. Colloid. Interface. Sci.*, 2019, **541**, 356-366.
- L. Jiang, X. Yuan, G. Zeng, J. Liang, Z. Wu, H. Yu, D. Mo, H. Wang, Z. Xiao and C. Zhou, *J. Colloid. Interface. Sci.*, 2019, **536**, 17-29.
- Z. M. Zhang, T. Zhang, C. Wang, Z. Lin, L. S. Long and W. Lin, *J. Am. Chem. Soc.*, 2015, **137**, 3197-3200.
- X.-J. Kong, Z. Lin, Z.-M. Zhang, T. Zhang and W. Lin, *Angew. Chem. Int. Ed.*, 2016, **55**, 6411-6416.
- J. J. Walsh, A. M. Bond, R. J. Forster and T. E. Keyes, *Coord. Chem. Rev.*, 2016, **306**, 217-234.
- D. Huang, X. Yan, M. Yan, G. Zeng, C. Zhou, J. Wan, M. Cheng and W. Xue, *ACS Appl. Mater. Inter.*, 2018, **10**, 21035-21055.
- W. Xue, D. Huang, J. Li, G. Zeng, R. Deng, Y. Yang, S. Chen, Z. Li, X. Gong and B. Li, *Chem. Eng. J.*, 2019, **373**, 1144-1157.
- D. Huang, Z. Li, G. Zeng, C. Zhou, W. Xue, X. Gong, X. Yan, S. Chen, W. Wang and M. Cheng, *Appl. Catal. B*, 2019, **240**, 153-173.
- Y. Liu, M. Cheng, Z. Liu, G. Zeng, H. Zhong, M. Chen, C. Zhou, W. Xiong, B. Shao and B. Song, *Chemosphere*, 2019, **236**, 124387.
- T. Xu, X. Liu, S. Wang and L. Li, *Nano-Micro Letters*, 2019, **11**, 37.
- P. Sudarsanam, E. Peeters, E. V. Makshina, V. I. Parvulescu and B. F. Sels, *Chem. Soc. Rev.*, 2019, **48**, 2366-2421.
- R. J. White, R. Luque, V. L. Budarin, J. H. Clark and D. J. Macquarrie, *Chem. Soc. Rev.*, 2009, **38**, 481-494.
- B. H. Wu and N. F. Zheng, *Nano Today*, 2013, **8**, 168-197.
- L. Chen, Y. Honscho, S. Seki and D. L. Jiang, *J. Am. Chem. Soc.*, 2010, **132**, 6742-6748.
- H. Wang, Z. Zeng, P. Xu, L. Li, G. Zeng, R. Xiao, Z. Tang, D. Huang, L. Tang, C. Lai, D. Jiang, Y. Liu, H. Yi, L. Qin, S. Ye, X. Ren and W. Tang, *Chem. Soc. Rev.*, 2019, **48**, 488-516.
- T. Xu, S. Wang, L. Li and X. Liu, *Applied Catalysis A: General*, 2019, **575**, 132-141.
- S. Linic, P. Christopher and D. B. Ingram, *Nat. Mater.*, 2011, **10**,

- 911-921.
49. C.-C. Wang, J.-R. Li, X.-L. Lv, Y.-Q. Zhang and G. Guo, *Energy Environ. Sci.*, 2014, **7**, 2831-2867.
50. T. Zhang and W. Lin, *Chem. Soc. Rev.*, 2014, **43**, 5982-5993.
51. T. Banerjee, K. Gottschling, G. Savasci, C. Ochsenfeld and B. V. Lotsch, *ACS Energy Letters*, 2018, **3**, 400-409.
52. J. X. Jiang, F. Su, A. Trewin, C. D. Wood, N. L. Campbell, H. Niu, C. Dickinson, A. Y. Ganin, M. J. Rosseinsky, Y. Z. Khimyak and A. I. Cooper, *Angew. Chem. Int. Ed.*, 2007, **46**, 8574-8578.
53. Y. Xu, S. Jin, H. Xu, A. Nagai and D. Jiang, *Chem. Soc. Rev.*, 2013, **42**, 8012-8031.
54. G. Zhang, Z.-A. Lan and X. Wang, *Angew. Chem. Int. Ed.*, 2016, **55**, 15712-15727.
55. K. Zhang, Z. Vobecka, K. Tauer, M. Antonietti and F. Vilela, *Chem. Commun.*, 2013, **49**, 11158-11160.
56. J. X. Jiang, Y. Y. Li, X. F. Wu, J. L. Xiao, D. J. Adams and A. I. Cooper, *Macromolecules*, 2013, **46**, 8779-8783.
57. Z. J. Wang, S. Ghasimi, K. Landfester and K. A. Zhang, *Chem. Commun.*, 2014, **50**, 8177-8180.
58. Z. J. Wang, S. Ghasimi, K. Landfester and K. A. I. Zhang, *J. Mater. Chem. A*, 2014, **2**, 18720-18724.
59. M. Sener, J. Strumpfer, J. Hsin, D. Chandler, S. Scheuring, C. N. Hunter and K. Schulten, *Chemphyschem*, 2011, **12**, 518-531.
60. M. K. Sener, J. D. Olsen, C. N. Hunter and K. Schulten, *PNAS*, 2007, **104**, 15723-15728.
61. M. Sener, J. Strumpfer, J. A. Timney, A. Freiberg, C. N. Hunter and K. Schulten, *Biophys. J.*, 2010, **99**, 67-75.
62. R. P. Goncalves, J. Busselez, D. Levy, J. Seguin and S. Scheuring, *J. Struct. Biol.*, 2005, **149**, 79-86.
63. C. Uragai, Y. Sugai, K. Hanjo, A. Sumino, R. Fujii, T. Nishioka, I. Kinoshita, T. Dewa, M. Nango, A. T. Gardiner, R. J. Cogdell and H. Hashimoto, *J. Photochem. Photobiol. A: Chem.*, 2015, **313**, 60-71.
64. D. Murat, M. Byrne and A. Komeili, *Cold Spring Harb. Perspect. Biol.*, 2010, **2**, a000422.
65. J. Hsin, J. Strumpfer, M. Sener, P. Qian, C. N. Hunter and K. Schulten, *New J. Phys.*, 2010, **12**, 085005.
66. L. Chen, Y. Honsho, S. Seki and D. Jiang, *J. Am. Chem. Soc.*, 2011, **133**, 6742-6748.
67. K. V. Rao, R. Haldar, T. K. Maji and S. J. George, *PCCP*, 2016, **18**, 156-163.
68. B. G. Kim, X. Ma, C. Chen, Y. Je, E. W. Coir, H. Hashemi, Y. Aso, P. F. Green, J. Kieffer and J. Kim, *Adv. Funct. Mater.*, 2013, **23**, 439-445.
69. B. Keller, A. McLean, B. G. Kim, K. Chung, J. Kim and T. Goodson, *J. Phys. Chem. C*, 2016, **120**, 9088-9096.
70. A. Casey, S. D. Dimitrov, P. Shakya-Tuladhar, Z. P. Fei, M. Nguyen, Y. Han, T. D. Anthopoulos, J. R. Durrant and M. Heeney, *Chem. Mater.*, 2016, **28**, 5110-5120.
71. Y. Y. Yu, T. W. Tsai and C. P. Chen, *J. Phys. Chem. C*, 2018, **122**, 24585-24591.
72. R. H. Friend, R. W. Gymer, A. B. Holmes, J. H. Burroughes, R. N. Marks, C. Taliani, D. D. C. Bradley, D. A. D. Santos, J. L. Brédas, M. Lögdlund and W. R. Salaneck, *Nature*, 1999, **397**, 121-128.
73. A. J. Berresheim, M. Muller and K. Mullen, *Chem. Rev.*, 1999, **99**, 1747-1786.
74. U. H. Bunz, *Chem. Rev.*, 2000, **100**, 1605-1644.
75. U. Scherf and E. J. W. List, *Adv. Mater.*, 2002, **14**, 477-487.
76. J. X. Jiang, F. Su, H. Niu, C. D. Wood, N. L. Campbell, Y. Z. Khimyak and A. I. Cooper, *Chem. Commun.*, 2008, DOI: 10.1039/b715563h, 486-488.
77. J. X. Jiang, F. Su, A. Trewin, C. D. Wood, H. Niu, J. T. Jones, Y. Z. Khimyak and A. I. Cooper, *J. Am. Chem. Soc.*, 2008, **130**, 7710-7720.
78. J. Weber and A. Thomas, *J. Am. Chem. Soc.*, 2008, **130**, 6334-6335.
79. A. I. Cooper, *Adv. Mater.*, 2009, **21**, 1291-1295.
80. J. Schmidt, M. Werner and A. Thomas, *Macromolecules*, 2009, **42**, 4426-4429.
81. Z. J. Wang, S. Ghasimi, K. Landfester and K. A. Zhang, *Adv. Mater.*, 2015, **27**, 6265-6270.
82. J. Schmidt, J. Weber, J. D. Epping, M. Antonietti and A. Thomas, *Adv. Mater.*, 2009, **21**, 702-705.
83. Y. Xu, L. Chen, Z. Guo, A. Nagai and D. Jiang, *J. Am. Chem. Soc.*, 2011, **133**, 17622-17625.
84. G. Cheng, T. Hasell, A. Trewin, D. J. Adams and A. I. Cooper, *Angew. Chem. Int. Ed.*, 2012, **51**, 12727-12731.
85. Y. Xu, A. Nagai and D. Jiang, *Chem. Commun.*, 2013, **49**, 1591-1593.
86. C. Gu, N. Huang, J. Gao, F. Xu, Y. Xu and D. Jiang, *Angew. Chem. Int. Ed.*, 2014, **53**, 4850-4855.
87. B. Bonillo, R. S. Sprick and A. I. Cooper, *Chem. Mater.*, 2016, **28**, 3469-3480.
88. X. Li, Z. Li and Y. W. Yang, *Adv. Mater.*, 2018, **30**, 1800177.
89. Y. Xu, N. Mao, S. Feng, C. Zhang, F. Wang, Y. Chen, J. Zeng and J.-X. Jiang, *Macromol. Chem. Phys.*, 2017, **218**, 1700049.
90. Y. Xu, C. Zhang, M. H. Ma, X. Wang, Q. He, F. Wang and J.-X. Jiang, *Science China-Chemistry*, 2017, **60**, 1075-1083.
91. C. Yang, B. C. Wu, L. Zhang, S. Lin, S. Ghasimi, K. Landfester, K. A. Zhang and X. Wang, *Angew. Chem. Int. Ed.*, 2016, **55**, 9202-9205.
92. K. Zhang, D. Kopetzki, P. H. Seeberger, M. Antonietti and F. Vilela, *Angew. Chem. Int. Ed.*, 2013, **52**, 1432-1436.
93. M. Schrab, M. Hamburger, X. Feng, J. Shu, H. W. Spiess, X. Wang, M. Antonietti and K. Mullen, *Chem. Commun.*, 2010, **46**, 8931-8934.
94. J. X. Jiang, A. Trewin, D. J. Adams and A. I. Cooper, *Chem. Sci.*, 2011, **2**, 1777-1781.
95. L. Li, Z. Cai, Q. Wu, W. Y. Lo, N. Zhang, L. X. Chen and L. Yu, *J. Am. Chem. Soc.*, 2016, **138**, 7681-7686.
96. Y. Xu, N. Mao, C. Zhang, X. Wang, J. Zeng, Y. Chen, F. Wang and J.-X. Jiang, *Appl. Catal. B*, 2018, **228**, 1-9.
97. L. Li, W.-y. Lo, Z. Cai, N. Zhang and L. Yu, *Macromolecules*, 2016, **49**, 6903-6909.
98. K. Kailasam, M. B. Mesch, L. Mohlmann, M. Baar, S. Blechert, M. Schwarze, M. Schroder, R. Schomacker, J. Senker and A. Thomas, *Energy Technology*, 2016, **4**, 744-750.
99. R. S. Sprick, J. X. Jiang, B. Bonillo, S. Ren, T. Ratvijitvech, P. Guignon, M. A. Zwijnenburg, D. J. Adams and A. I. Cooper, *J. Am. Chem. Soc.*, 2015, **137**, 3265-3270.
100. P. B. Pati, G. Damas, L. Tian, D. L. A. Fernandes, L. Zhang, I. B. Pehlivan, T. Edvinsson, C. M. Araujo and H. N. Tian, *Energy Environ. Sci.*, 2017, **10**, 1372-1376.
101. C. Gu, Y. Chen, Z. Zhang, S. Xue, S. Sun, K. Zhang, C. Zhong, H. Zhang, Y. Pan, Y. Lv, Y. Yang, F. Li, S. Zhang, F. Huang and Y. Ma, *Adv. Mater.*, 2013, **25**, 3443-3448.
102. C. Gu, N. Huang, Y. Chen, L. Qin, H. Xu, S. Zhang, F. Li, Y. Ma and D. Jiang, *Angew. Chem. Int. Ed.*, 2015, **54**, 13594-13598.
103. F. Wei, X. Cai, J. Nie, F. Wang, C. Lu, G. Yang, Z. Chen, C. Ma and Y. Zhang, *Polym. Chem.*, 2018, **9**, 3832-3839.
104. Y. Liu, Z. Liao, X. Ma and Z. Xiang, *ACS Appl. Mater. Inter.*, 2018, **10**, 30698-30705.
105. W.-Y. Huang, Z.-Q. Shen, J.-Z. Cheng, L.-L. Liu, K. Yang, X. Chen, H.-R. Wen and S.-Y. Liu, *J. Mater. Chem. A*, 2019, **7**, 24222-24230.
106. H.-J. Hou, X.-H. Zhang, D.-K. Huang, X. Ding, S.-Y. Wang, X.-L.

- Yang, S.-Q. Li, Y.-G. Xiang and H. Chen, *Appl. Catal. B*, 2017, **203**, 563-571.
107. J. Chen, X. Tao, L. Tao, H. Li, C. Li, X. Wang, C. Li, R. Li and Q. Yang, *Appl. Catal. B*, 2019, **241**, 461-470.
108. K. Maeda, *ACS Catal.*, 2013, **3**, 1486-1503.
109. T. Hisatomi, J. Kubota and K. Domen, *Chem. Soc. Rev.*, 2014, **43**, 7520-7535.
110. J. Ran, J. Zhang, J. Yu, M. Jaroniec and S. Z. Qiao, *Chem. Soc. Rev.*, 2014, **43**, 7787-7812.
111. Y. F. Zhao, B. Li, Q. Wang, W. Gao, C. L. J. Wang, M. Wei, D. G. Evans, X. Duan and D. O'Hare, *Chem. Sci.*, 2014, **5**, 951-958.
112. S. J. A. Moniz, S. A. Shevlin, D. J. Martin, Z.-X. Guo and J. Tang, *Energy Environ. Sci.*, 2015, **8**, 731-759.
113. Y. F. Zhao, X. D. Jia, G. I. N. Waterhouse, L. Z. Wu, C. H. Tung, D. O'Hare and T. R. Zhang, *Adv. Energy Mater.*, 2016, **6**, 1501974.
114. M. Karayilan, W. P. Brezinski, K. E. Clary, D. L. Lichtenberger, R. S. Glass and J. Pyun, *Angew. Chem. Int. Ed.*, 2019, **131**, 7617-7630.
115. K. Mazloomi and C. Gomes, *Renew. Sust. Energ. Rev.*, 2012, **16**, 3024-3033.
116. J. Chen, X. P. Tao, L. Tao, H. Li, C. Z. Li, X. L. Wang, C. Li, R. G. Li and Q. H. Yang, *Appl. Catal. B*, 2019, **241**, 461-470.
117. Z. A. Lan, W. Ren, X. Chen, Y. F. Zhang and X. C. Wang, *Appl. Catal. B*, 2019, **245**, 596-603.
118. L. Schlapbach and A. Züttel, *Nature*, 2001, **414**, 353-358.
119. N. S. Lewis and D. G. Nocera, *PNAS*, 2006, **103**, 15729-15735.
120. A. W. C. van den Berg and C. O. Areán, *Chem. Commun.*, 2008, DOI: 10.1039/b712576n, 668-681.
121. P. Jena, *J. Phys. Chem. Lett.*, 2011, **2**, 206-211.
122. G. Zhang, Z. A. Lan and X. Wang, *Angew. Chem. Int. Ed.*, 2016, **55**, 15712-15727.
123. H. Wang, B. Hou, Y. Yang, Q. Chen, M. Zhu, A. Thomas and Y. Liao, *Small*, 2018, **14**, 1803232.
124. V. S. Mothika, P. Sutar, P. Verma, S. Das, S. K. Pati and T. K. Maji, *Chemistry (Easton)*, 2019, **25**, 3867-3874.
125. G. Q. Zhang, W. Ou, J. Wang, Y. S. Xu, D. Xu, T. Sun, S. A. Xiao, M. R. Wang, H. X. Li, W. Chen and C. L. Su, *Appl. Catal. B*, 2019, **245**, 114-121.
126. K. Ding, Q. Zhang, Q. Li and S. Ren, *Macromol. Chem. Phys.*, 2019, **220**, 1900304.
127. C. Cheng, X. Wang, Y. Lin, L. He, J.-X. Jiang, Y. Xu and F. Wang, *Polym. Chem.*, 2018, **9**, 4468-4475.
128. A. Bhunia, D. Esquivel, S. Desai, R. Fernandez Feran, Y. Goto, S. Inagaki, P. Van der Voort and C. Lamark, *J. Mater. Chem. A*, 2016, **4**, 13450-13457.
129. G. Zhang, W. Ou, J. Wang, Y. Xu, D. Xu, T. Sun, S. Xiao, M. Wang, H. Li, W. Chen and C. Su, *Appl. Catal. B*, 2019, **245**, 114-121.
130. C. B. Meier, R. S. Sprick, A. Monti, P. Guiglion, J.-S. M. Lee, M. A. Zwijnenburg and A. I. Cooper, *Polymer*, 2017, **126**, 283-290.
131. C. Cheng, X. Wang and F. Wang, *Appl. Surf. Sci.*, 2019, **495**, 143537.
132. J. Yu, X. Sun, X. Xu, C. Zhang and X. He, *Appl. Catal. B*, 2019, **257**, 117935.
133. L. Guo, Y. Niu, S. Razzaque, B. Tan and S. Jin, *ACS Catal.*, 2019, **9**, 9438-9445.
134. K. Lin, Z. Wang, Z. Hu, P. Luo, X. Yang, X. Zhang, M. Rafiq, F. Huang and Y. Cao, *J. Mater. Chem. A*, 2019, **7**, 19087-19093.
135. R. S. Sprick, Y. Bai, A. A. Y. Guilbert, M. Zbiri, C. M. Aitchison, L. Wilbraham, Y. Yan, D. J. Woods, M. A. Zwijnenburg and A. I. Cooper, *Chem. Mater.*, 2019, **31**, 305-313.
136. L. Guo, Y. Niu, H. Xu, Q. Li, S. Razzaque, Q. Huang, S. Jin and B. Tan, *J. Mater. Chem. A*, 2018, **6**, 19775-19781.
137. S. Bi, Z.-A. Lan, S. Paasch, W. Zhang, Y. He, C. Zhang, F. Liu, D. Wu, X. Zhuang, E. Brunner, X. Wang and F. Zhang, *Adv. Funct. Mater.*, 2017, **27**, 1703146.
138. D. Schwarz, Y. S. Kochergin, A. Acharjya, A. Ichangi, M. V. Opanasenko, J. Cejka, U. Lappan, P. Arki, J. He, J. Schmidt, P. Nachtigall, A. Thomas, J. Tarabek and M. J. Bojdys, *Chemistry-a European Journal*, 2017, **23**, 13023-13027.
139. M. G. Schwab, M. Hamburger, X. Feng, J. Shu, H. W. Spiess, X. Wang, M. Antonietti and K. Müllen, *Chem. Commun.*, 2010, **46**, 8932-8934.
140. R. S. Sprick, J.-X. Jiang, B. Bonillo, S. Ren, T. Ratvijitvech, P. Guiglion, M. A. Zwijnenburg, D. J. Adams and A. I. Cooper, *J. Am. Chem. Soc.*, 2015, **137**, 3265-3270.
141. J. Cai, P. Ruffieux, R. Jaafar, M. Bieri, T. Braun, S. Blankenburg, M. Muoth, A. P. Seitsonen, M. Saleh, X. Feng, K. Müllen and R. Fasel, *Nature*, 2010, **466**, 470-473.
142. R. S. Sprick, B. Bonillo, M. Sachs, R. Clowes, J. R. Durrant, D. J. Adams and A. I. Cooper, *Chem. Commun.*, 2016, **52**, 10008-10011.
143. K. V. Rao, S. Mohapatra, C. Kulkarni, T. K. Maji and S. J. George, *J. Mater. Chem.*, 2011, **21**, 12958-12963.
144. A. Modak, K. Yamanaka, Y. Goto and S. Inagaki, *Bull. Chem. Soc. Jpn.*, 2016, **89**, 887-891.
145. A. Modak, Y. Maegawa, Y. Goto and S. Inagaki, *Polym. Chem.*, 2016, **7**, 1290-1296.
146. Y. F. Xu, C. Zhang, Y. Mu, N. Mao, X. Wang, Q. He, F. Wang and J. X. Jiang, *Sci. China Chem.*, 2017, **60**, 1075-1083.
147. Y. F. Xu, N. Mao, C. Zhang, C. Zhang, F. Wang, Y. Chen, J. H. Zeng and J. X. Jiang, *Macromol. Chem. Phys.*, 2017, **218**, 1700049.
148. Z. J. Wang, X. Y. Yang, T. J. Yang, Y. B. Zhao, F. Wang, Y. Chen, J. H. Zeng, Y. Yan, F. Huang and J. X. Jiang, *ACS Catal.*, 2018, **8**, 859-859.
149. Y. Bai, L. Wilbraham, B. J. Slater, M. A. Zwijnenburg, R. S. Sprick and A. I. Cooper, *J. Am. Chem. Soc.*, 2019, **141**, 9063-9071.
150. K. L. Materna, R. H. Crabtree and G. W. Brudvig, *Chem. Soc. Rev.*, 2017, **46**, 6099-6110.
151. D. Kong, Y. Zheng, M. Kobielski, Y. Wang, Z. Bai, W. Macyk, X. Wang and J. Tang, *Mater. Today*, 2018, **21**, 897-924.
152. R. Eisenberg and H. B. Gray, *Inorg. Chem.*, 2008, **47**, 1697-1699.
153. L. Duan, F. Bozoglian, S. Mandal, B. Stewart, T. Privalov, A. Llobet and L. Sun, *Nat. Chem.*, 2012, **4**, 418-423.
154. S. Jayanthi, D. V. S. Muthu, N. Jayaraman, S. Sampath and A. K. Sood, *Chemistryselect*, 2017, **2**, 4522-4532.
155. L. Wang, Y. Wan, Y. Ding, Y. Niu, Y. Xiong, X. Wu and H. Xu, *Nanoscale*, 2017, **9**, 4090-4096.
156. Z. Wang, C. Li and K. Domen, *Chem. Soc. Rev.*, 2019, **48**, 2109-2125.
157. S. Chen, T. Takata and K. Domen, *Nat. Rev. Mater.*, 2017, **2**, 17050.
158. L. Wang, Y. Zhang, L. Chen, H. Xu and Y. Xiong, *Adv. Mater.*, 2018, **30**, 1801955.
159. G. Zhang, Z.-A. Lan and X. Wang, *Chem. Sci.*, 2017, **8**, 5261-5274.
160. H. Yu, R. Shi, Y. Zhao, G. I. N. Waterhouse, L.-Z. Wu, C.-H. Tung and T. Zhang, *Adv. Mater.*, 2016, **28**, 9454-9477.
161. M. G. Walter, E. L. Warren, J. R. McKone, S. W. Boettcher, Q. Mi, E. A. Santori and N. S. Lewis, *Chem. Rev.*, 2011, **111**, 5815-5815.
162. K. Maeda and K. Domen, *The Journal of Physical Chemistry Letters*, 2010, **1**, 2655-2661.
163. L. Liao, Q. Zhang, Z. Su, Z. Zhao, Y. Wang, Y. Li, X. Lu, D. Wei, G. Feng, Q. Yu, X. Cai, J. Zhao, Z. Ren, H. Fang, F. Robles-Hernandez, S. Baldelli and J. Bao, *Nat. Nanotechnol.*, 2014, **9**, 69-73.
164. J. Liu, Y. Liu, N. Liu, Y. Han, X. Zhang, H. Huang, Y. Lifshitz, S.-T. Lee, J. Zhong and Z. Kang, *Science*, 2015, **347**, 970.
165. K. Maeda, T. Takata, M. Hara, N. Saito, Y. Inoue, H. Kobayashi

- and K. Domen, *J. Am. Chem. Soc.*, 2005, **127**, 8286-8287.
166. V. S. Vyas, V. W.-h. Lau and B. V. Lotsch, *Chem. Mater.*, 2016, **28**, 5191-5204.
  167. V. S. Vyas, F. Haase, L. Stegbauer, G. Savasci, F. Podjaski, C. Ochsenfeld and B. V. Lotsch, *Nat. Commun.*, 2015, **6**, 8508.
  168. L. Li, Z. Cai, Q. Wu, W.-Y. Lo, N. Zhang, L. X. Chen and L. Yu, *J. Am. Chem. Soc.*, 2016, **138**, 7681-7686.
  169. V. S. Vyas and B. V. Lotsch, *Nature*, 2015, **521**, 41-42.
  170. R. S. Sprick, B. Bonillo, R. Clowes, P. Guiglion, N. J. Brownbill, B. J. Slater, F. Blanc, M. A. Zwijnenburg, D. J. Adams and A. I. Cooper, *Angew. Chem. Int. Ed.*, 2016, **55**, 1792-1796.
  171. X. Wang, K. Maeda, A. Thomas, K. Takanabe, G. Xin, J. M. Carlsson, K. Domen and M. Antonietti, *Nat. Mater.*, 2009, **8**, 76-80.
  172. J. Wirth, R. Neumann, M. Antonietti and P. Saalfrank, *PCCP*, 2014, **16**, 15917-15926.
  173. D. J. Martin, P. J. T. Reardon, S. J. A. Moniz and J. Tang, *J. Am. Chem. Soc.*, 2014, **136**, 12568-12571.
  174. S. Yang, Y. Gong, J. Zhang, L. Zhan, L. Ma, Z. Fang, R. Vajtai, X. Wang and P. M. Ajayan, *Adv. Mater.*, 2013, **25**, 2452-2456.
  175. K. Schwinghammer, M. B. Mesch, V. Duppel, C. Ziegler, J. Senker and B. V. Lotsch, *J. Am. Chem. Soc.*, 2014, **136**, 1730-1733.
  176. L. Wang, Y. Wan, Y. Ding, S. Wu, Y. Zhang, X. Zhang, G. Zhang, Y. Xiong, X. Wu, J. Yang and H. Xu, *Adv. Mater.*, 2017, **29**, 1702428.
  177. J. Zhou, X. Gao, R. Liu, Z. Xie, J. Yang, S. Zhang, G. Zhang, H. Liu, Y. Li, J. Zhang and Z. Liu, *J. Am. Chem. Soc.*, 2015, **137**, 7596-7599.
  178. G. Zhang, Z.-A. Lan, L. Lin, S. Lin and X. Wang, *Chem. Sci.*, 2016, **7**, 3062-3066.
  179. K. C. Nicolaou, Y. H. Lim and J. Becker, *Angew. Chem. Int. Ed.*, 2009, **48**, 3444-3448.
  180. Y. Liu, Y. Yang, Q. Sun, Z. Wang, B. Huang, Y. Dai, X. Qin and X. Zhang, *ACS Appl. Mater. Inter.*, 2013, **5**, 7654-7658.
  181. A. Listorti, J. Durrant and J. Barber, *Nat. Mater.*, 2009, **8**, 929-930.
  182. O. K. Varghese, M. Paulose, T. J. Latempa and C. A. Grimes, *Nano Lett.*, 2009, **9**, 731-737.
  183. Y. Izumi, *Coord. Chem. Rev.*, 2013, **257**, 171-186.
  184. W. Tu, Y. Zhou and Z. Zou, *Adv. Mater.*, 2014, **26**, 4647-4656.
  185. S. Bandyopadhyay, A. G. Anil, A. James and A. Patra, *ACS Appl. Mater. Inter.*, 2016, **8**, 27669-27678.
  186. I. Omae, *Catal. Today*, 2006, **115**, 33-42.
  187. M. Vogt, M. Gargir, M. A. Iron, A. Diskin Posner, Y. Ben-David and D. Milstein, *Chemistry (Easton)*, 2018, **18**, 9194-9197.
  188. C. A. Huff, J. W. Kampf and M. S. Sanford, *Organometallics*, 2012, **31**, 4643-4645.
  189. F. M. Wissler, P. Berruyer, L. Cardenas, Y. Mohr, E. A. Quadrelli, A. Lesage, D. Farrusseng and J. Canivet, *ACS Catal.*, 2018, **8**, 1653-1661.
  190. C. Yang, W. Huang, L. C. da Silva, K. A. I. Zhang and X. Wang, *Chemistry (Easton)*, 2018, **24**, 17454-17458.
  191. X. Yu, Z. Yang, B. Qiu, S. Guo, P. Yang, B. Yu, H. Zhang, Y. Zhao, X. Yang, B. Han and Z. Liu, *Angew. Chem. Int. Ed.*, 2019, **58**, 632-636.
  192. H. Zhong, Z. Hong, C. Yang, L. Li, Y. Xu, X. Wang and R. Wang, *Chemsuschem*, 2019, **12**, 4529-4537.
  193. V. A. Montes, C. Pérez-Bolívar, N. Agarwal, J. Shinar and P. Anzenbacher, *J. Am. Chem. Soc.*, 2006, **128**, 12436-12438.
  194. X. Huang, C. Zhu, S. Zhang, W. Li, Y. Guo, X. Zhan, Y. Liu and Z. Bo, *Macromolecules*, 2008, **41**, 6895-6902.
  195. R. Ambre, K.-B. Chen, C.-F. Yao, L. Luo, E. W.-G. Diau and C.-H. Hung, *The Journal of Physical Chemistry C*, 2012, **116**, 11907-11916.
  196. J. Grodkowski, D. Behar, P. Neta and P. Hambright, *The Journal of Physical Chemistry A*, 1997, **101**, 248-254.
  197. D. Behar, T. Dhanasekaran, P. Neta, C. M. Hosten, D. Ejeh, P. Hambright and E. Fujita, *The Journal of Physical Chemistry A*, 1998, **102**, 2870-2877.
  198. K. Leung, I. M. B. Nielsen, N. Sai, C. Medforth and J. A. Shelnutt, *The Journal of Physical Chemistry A*, 2010, **114**, 10174-10184.
  199. I. Hod, M. D. Sampson, P. Deria, C. P. Kubiak, O. K. Farha and J. T. Hupp, *ACS Catal.*, 2015, **5**, 6302-6309.
  200. X. Zhan, Z. a. Tan, B. Domercq, Z. An, X. Zhang, S. Barlow, Y. Li, D. Zhu, B. Kippelen and S. R. Marder, *J. Am. Chem. Soc.*, 2007, **129**, 7246-7247.
  201. K. Kunal, C. G. Robertson, S. Pawlus, S. F. Hahn and A. P. Sokolov, *Macromolecules*, 2008, **41**, 7232-7238.
  202. C. Cui, W.-Y. Wong and Y. Li, *Energy Environ. Sci.*, 2014, **7**, 2276-2284.
  203. C. Chen, C. Tang, W. Xu, Y. Li and L. Xu, *PCCP*, 2018, **20**, 9536-9542.
  204. L. Shi and W. Xia, *Chem. Soc. Rev.*, 2012, **41**, 7687-7697.
  205. J. Xuan and W.-J. Xiao, *Angew. Chem. Int. Ed.*, 2012, **51**, 6828-6838.
  206. M. Rueping, C. Vila, A. Szadkowska, R. M. Koenigs and J. Fronert, *ACS Catal.*, 2012, **2**, 2810-2815.
  207. C. K. Prier, D. A. Rankin and D. W. C. MacMillan, *Chem. Rev.*, 2013, **113**, 5322-5363.
  208. D. M. Schultz and T. P. Moon, *Science*, 2014, **343**, 1239176.
  209. L. Qin, H. Yi, G. Zeng, C. Lai, D. Huang, P. Xu, Y. Fu, J. He, B. Li and C. Zhang, *J. Hazard. Mater.*, 2019, **380**, 120864.
  210. L. Qin, G. Zeng, G. Zeng, C. Lai, A. Duan, R. Xiao, D. Huang, Y. Fu, H. Yi and B. Li, *Appl. Catal. B*, 2019, **259**, 118035.
  211. Y. F. Zhi, K. Li, H. Xia, M. Xue, Y. Mu and X. M. Liu, *J. Mater. Chem. A*, 2017, **5**, 8697-8704.
  212. C. Ayed, L. C. da Silva, D. Wang and K. A. I. Zhang, *J. Mater. Chem. A*, 2018, **6**, 22145-22151.
  213. Y. F. Zhi, S. Ma, H. Xia, Y. M. Zhang, Z. Shi, Y. Mu and X. M. Liu, *Appl. Catal. B*, 2019, **244**, 36-44.
  214. C. Monterde, R. Navarro, M. Iglesias and F. Sanchez, *ACS Appl. Mater. Inter.*, 2019, **11**, 3459-3465.
  215. W. Ou, G. Q. Zhang, J. Wu and C. L. Su, *ACS Catal.*, 2019, **9**, 5178-5183.
  216. J. Luo, X. Zhang and J. Zhang, *ACS Catal.*, 2015, **5**, 2250-2254.
  217. Y. Zhi, K. Li, H. Xia, M. Xue, Y. Mu and X. M. Liu, *J. Mater. Chem. A*, 2017, **5**, 8697-8704.
  218. C. Ayed, W. Huang, R. Li, L. C. da Silva, D. Wang, O. Suraeva, W. Najjar and K. A. I. Zhang, *Particle & Particle Systems Characterization*, 2018, **35**, 1700234.
  219. H. Bohra, P. Li, C. Yang, Y. Zhao and M. Wang, *Polym. Chem.*, 2018, **9**, 1972-1982.
  220. W. Liu, S. Wu, Q. Su, B. Guo, P. Ju, G. Li and Q. Wu, *Journal of Materials Science*, 2019, **54**, 1205-1212.
  221. H. Zhang, Q. Huang, W. Zhang, C. Pan, J. Wang, C. Ai, J. Tang and G. Yu, *Chemphotochem*, 2019, **3**, 645-651.
  222. Z. J. Wang, R. Li, K. Landfester and K. A. I. Zhang, *Polymer*, 2017, **126**, 291-295.
  223. C.-A. Wang, Y.-W. Li, X.-L. Cheng, J.-P. Zhang and Y.-F. Han, *Rsc Advances*, 2017, **7**, 408-414.
  224. S. Ghasimi, S. A. Bretschneider, W. Huang, K. Landfester and K. A. I. Zhang, *Adv. Sci.*, 2017, **4**, 1700101.
  225. Y. Zhi, S. Ma, H. Xia, Y. Zhang, Z. Shi, Y. Mu and X. M. Liu, *Appl. Catal. B*, 2019, **244**, 36-44.
  226. X. Ding and B. H. Han, *Angew. Chem. Int. Ed.*, 2015, **54**, 6536-6539.
  227. N. Boens, V. Leen and W. Dehaen, *Chem. Soc. Rev.*, 2012, **41**,

- 1130-1172.
228. A. Kamkaew, S. H. Lim, H. B. Lee, L. V. Kiew, L. Y. Chung and K. Burgess, *Chem. Soc. Rev.*, 2013, **42**, 77-88.
229. H. Lu, J. Mack, Y. Yang and Z. Shen, *Chem. Soc. Rev.*, 2014, **43**, 4778-4823.
230. Y. Ni and J. Wu, *Org. Biomol. Chem.*, 2014, **12**, 3774-3791.
231. J. M. Tobin, J. Liu, H. Hayes, M. Demleitner, D. Ellis, V. Arrighi, Z. Xu and F. Vilela, *Polym. Chem.*, 2016, **7**, 6662-6670.
232. M. Liras, M. Iglesias and F. Sanchez, *Macromolecules*, 2016, **49**, 1666-1673.
233. Z. J. Wang, S. Ghasimi, K. Landfester and K. A. I. Zhang, *Chem. Mater.*, 2015, **27**, 1921-1924.
234. W. J. Zhang, J. T. Tang, W. G. Yu, Q. Huang, Y. Fu, G. C. Kuang, C. Y. Pan and G. P. Yu, *ACS Catal.*, 2018, **8**, 8084-8091.
235. V. R. Battula, H. Singh, S. Kumar, I. Bala, S. K. Pal and K. Kailasam, *ACS Catal.*, 2018, **8**, 6751-6759.
236. B. Song, G. Zeng, J. Gong, J. Liang, P. Xu, Z. Liu, Y. Zhang, C. Zhang, M. Cheng, Y. Liu, S. Ye, H. Yi and X. Ren, *Environ. Int.*, 2017, **105**, 43-55.
237. X. Y. Ren, G. M. Zeng, L. Tang, J. J. Wang, J. Wan, H. P. Feng, B. Song, C. Huang and X. Tang, *Soil Biol. Biochem.*, 2018, **116**, 70-81.
238. D. Hu, M. Shen, Y. Zhang and G. Zeng, *Sci. Total Environ.*, 2019, **657**, 108-110.
239. B. Shao, X. Liu, Z. Liu, G. Zeng, W. Zhang, Q. Liang, Y. Liu, Q. He, X. Yuan, D. Wang, S. Luo and S. Gong, *Chem. Eng. J.*, 2019, **374**, 479-493.
240. Y. Fu, P. Xu, D. Huang, G. Zeng, C. Lai, L. Qin, B. Li, J. He, H. Yi, M. Cheng and C. Zhang, *Appl. Surf. Sci.*, 2019, **473**, 578-588.
241. S. Tonda, S. Kumar, S. Kandula and V. Shanker, *J. Mater. Chem. A*, 2014, **2**, 6772-6780.
242. K. He, G. Q. Chen, G. M. Zeng, A. W. Chen, Z. Z. Huang, J. B. Shi, T. T. Huang, M. Peng and L. Hu, *Appl. Catal. B*, 2018, **228**, 19-28.
243. L. Tang, Y. I. Liu, J. J. Wang, G. M. Zeng, Y. C. Deng, H. R. Dong, H. P. Feng, J. J. Wang and B. Peng, *Appl. Catal. B*, 2018, **231**, 1-10.
244. D. N. Jiang, M. Chen, H. Wang, G. M. Zeng, D. L. Huang, M. Cheng, Y. Liu, W. J. Xue and Z. W. Wang, *Coord. Chem. Rev.*, 2019, **380**, 471-483.
245. S. Ghasimi, S. Prescher, Z. J. Wang, K. Landfester, J. Yuan and K. A. I. Zhang, *Angew. Chem. Int. Ed.*, 2015, **54**, 14549-14553.
246. L. Li and Z. Cai, *Polym. Chem.*, 2016, **7**, 4937-4943.
247. Z. Xiao, Y. Zhou, X. Xin, Q. Zhang, L. Zhang, R. Wang and D. Sun, *Macromol. Chem. Phys.*, 2016, **217**, 99-104.
248. Y. Li, M. Liu and L. Chen, *J. Mater. Chem. A*, 2017, **5**, 13757-13762.
249. B. Wang, Z. Xie, Y. Li, Z. Yang and L. Chen, *Macromolecules*, 2018, **51**, 3443-3449.
250. J. Wang, H. Yang, L. Jiang, S. Liu, Z. Hao, J. Cheng and G. Ouyang, *Catal. Sci. Technol.*, 2018, **8**, 5024-5033.
251. M. Li, H. Zhao and Z.-Y. Lu, *Microporous Mesoporous Mater.*, 2019, **292**, 109774.
252. L. Ma, Y. Liu, Y. Liu, S. Jiang, P. Li, Y. Hao, P. Shao, A. Yin, X. Feng and B. Wang, *Angew. Chem. Int. Ed.*, 2019, **58**, 4221-4226.
253. C. H. A. Tsang, J. Tobin, J. Xuan, F. Vilela, H. Huang and D. Y. C. Leung, *Appl. Catal. B*, 2019, **240**, 50-63.
254. C. Yang, N. Han, W. Zhang, W. Wang, W. Li, B. Xia, C. Han, Z. Cui and X. Zhang, *Chem. Eng. J.*, 2019, **374**, 1382-1393.
255. Y. Wang, A. D. Zhou, Y. Jiang, X. Y. Chen and J. B. He, *Rsc Advances*, 2015, **5**, 37823-37829.
256. Q. Liang, M. Zhang, C. H. Liu, S. Xu and Z. Y. Li, *Appl. Catal., A*, 2016, **519**, 107-115.
257. W. Lu, T. Xu, Y. Wang, H. Hu, N. Li, X. Jiang and W. Chen, *Appl. Catal. B*, 2016, **180**, 20-28.
258. Q. Li, H. G. Wang, Y. H. Li, Y. W. Li and Q. Duan, *Dyes and Pigments*, 2018, **149**, 261-267.
259. B. C. Ma, S. Ghasimi, K. Landfester, F. Vilela and K. A. I. Zhang, *J. Mater. Chem. A*, 2015, **3**, 16064-16071.
260. Y. S. Li, M. X. Liu and L. Chen, *J. Mater. Chem. A*, 2017, **5**, 13757-13762.
261. L. Cai, Y. Li, Y. Li, H. Wang, Y. Yu, Y. Liu and Q. Duan, *J. Hazard. Mater.*, 2018, **348**, 47-55.
262. Y. W. Li, Q. Duan, H. G. Wang, B. Gao, N. N. Qiu and Y. H. Li, *J. Photochem. Photobiol. A: Chem.*, 2018, **356**, 370-378.
263. J. H. Wang, H. S. Yang, L. Jiang, S. Q. Liu, Z. P. Hao, J. Cheng and G. F. Ouyang, *Catal. Sci. Technol.*, 2018, **8**, 5024-5033.
264. J. S. Li, X. H. Wen, Q. J. Zhang and S. J. Ren, *Rsc Advances*, 2018, **8**, 34560-34565.
265. M. Bednarz, J. Lapin, R. McGillicuddy, K. M. Pelzer, G. S. Engel and G. B. Griffin, *J. Phys. Chem. C*, 2017, **121**, 5467-5479.
266. Y. G. Xiang, X. P. Wang, X. H. Zhang, H. J. Hou, K. Dai, Q. Y. Huang and H. Chen, *J. Mater. Chem. A*, 2018, **6**, 153-159.
267. X. Wang, Y. H. Liang, W. J. An, J. S. Hu, Y. F. Zhu and W. Q. Cui, *Appl. Catal. B*, 2017, **219**, 53-62.
268. Y. Guan, S. M. Wang, Y. Wang, C. Sun, Y. Huang, C. Liu and H. Y. Zhao, *Appl. Catal. B*, 2017, **209**, 329-338.
269. Y. Liu, Z. Liu, D. Huang, M. Cheng, G. Zeng, C. Lai, C. Zhang, C. Zhou, W. Wang, L. Jiang, H. Wang and B. Shao, *Coord. Chem. Rev.*, 2019, **380**, 473-478.
270. R. P. Schwarzenbach, B. I. Escher, K. Fenner, T. B. Hofstetter, C. A. Johnson, U. von Gunten and B. Wehrli, *Science*, 2006, **313**, 1072-1077.
271. P. Smit and F. E. Romesberg, *Nat. Chem. Biol.*, 2007, **3**, 549-556.
272. P. Chait, A. Craney and R. Kishony, *Nature*, 2007, **446**, 668-671.
273. P. E. Sudbery, *Nat. Rev. Microbiol.*, 2011, **9**, 737-748.
274. Q. Zhang, G. Lambert, D. Liao, H. Kim, K. Robin, C. K. Tung, N. Pourmand and R. H. Austin, *Science*, 2011, **333**, 1764-1767.
275. H. Urakami, K. Zhang and F. Vilela, *Chem. Commun.*, 2013, **49**, 2353-2355.
276. A. P. Castano, P. Mroz and M. R. Hamblin, *Nat. Rev. Cancer*, 2006, **6**, 535-545.
277. M. Gruner, L. Tuchscher, B. Löffler, D. Gonnissen, K. Riehemann, M. C. Staniford, U. Kynast and C. A. Strassert, *ACS Appl. Mater. Inter.*, 2015, **7**, 20965-20971.
278. B. C. Ma, S. Ghasimi, K. Landfester and K. A. I. Zhang, *J. Mater. Chem. B*, 2016, **4**, 5112-5118.
279. F. Wang, F. Ren, D. Ma, P. Mu, H. J. Wei, C. H. Xiao, Z. Q. Zhu, H. X. Sun, W. D. Liang, J. X. Chen, L. H. Chen and A. Li, *J. Mater. Chem. A*, 2018, **6**, 266-274.
280. S. Jiang, B. C. Ma, W. Huang, A. Kaltbeitzel, G. Kizisavas, D. Crespy, K. A. I. Zhang and K. Landfester, *Nanoscale Horiz.*, 2018, **3**, 439-446.
281. R. T. Woodward, L. A. Stevens, R. Dawson, M. Vijayaraghavan, T. Hasell, I. P. Silverwood, A. V. Ewing, T. Ratvijitvech, J. D. Exley, S. Y. Chong, F. Blanc, D. J. Adams, S. G. Kazarian, C. E. Snape, T. C. Drage and A. I. Cooper, *J. Am. Chem. Soc.*, 2014, **136**, 9028-9035.
282. P. Lindemann, A. Schade, L. Monnereau, W. Feng, K. Batra, H. Gliemann, P. Levkin, S. Brase, C. Woll and M. Tsotsalis, *J. Mater. Chem. A*, 2016, **4**, 6815-6818.
283. B. Kiskan and J. Weber, *ACS Macro Lett.*, 2012, **1**, 37-40.